AZIENDA OSPEDALIERO - UNIVERSITARIA
Città della Salute e della Scienza di Torino

DEPARTMENT OF ONCOLOGY
UNIVERSITY OF TURIN

International Centre for Theoretical Physics

May 11, 2017 Trieste, Italy

4DCT and 4DCBCT in IGRT

Christian Fiandra


Trentino
Alto
Adige
Friuli
Venezia
Giulia
Valle
d'Aosta
Lombardia
Veneto
Emilia Romagna
Liguria
Toscana
Umbria
Lazio
Abruzzo
Molise
Campania
Puglia
Basilicata
Calabria
Sardegna
Sicilia

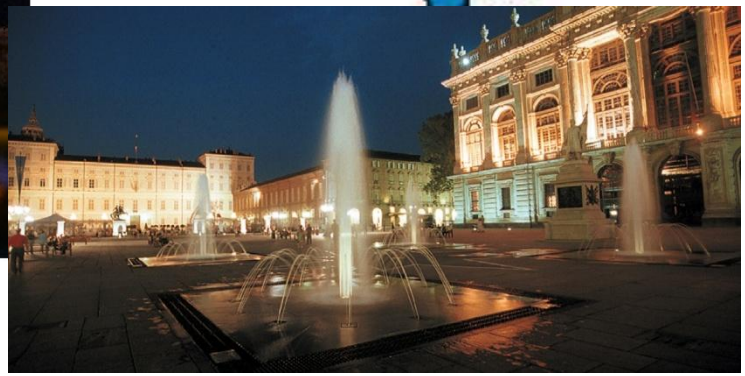

Radiation Oncology – University of Turin

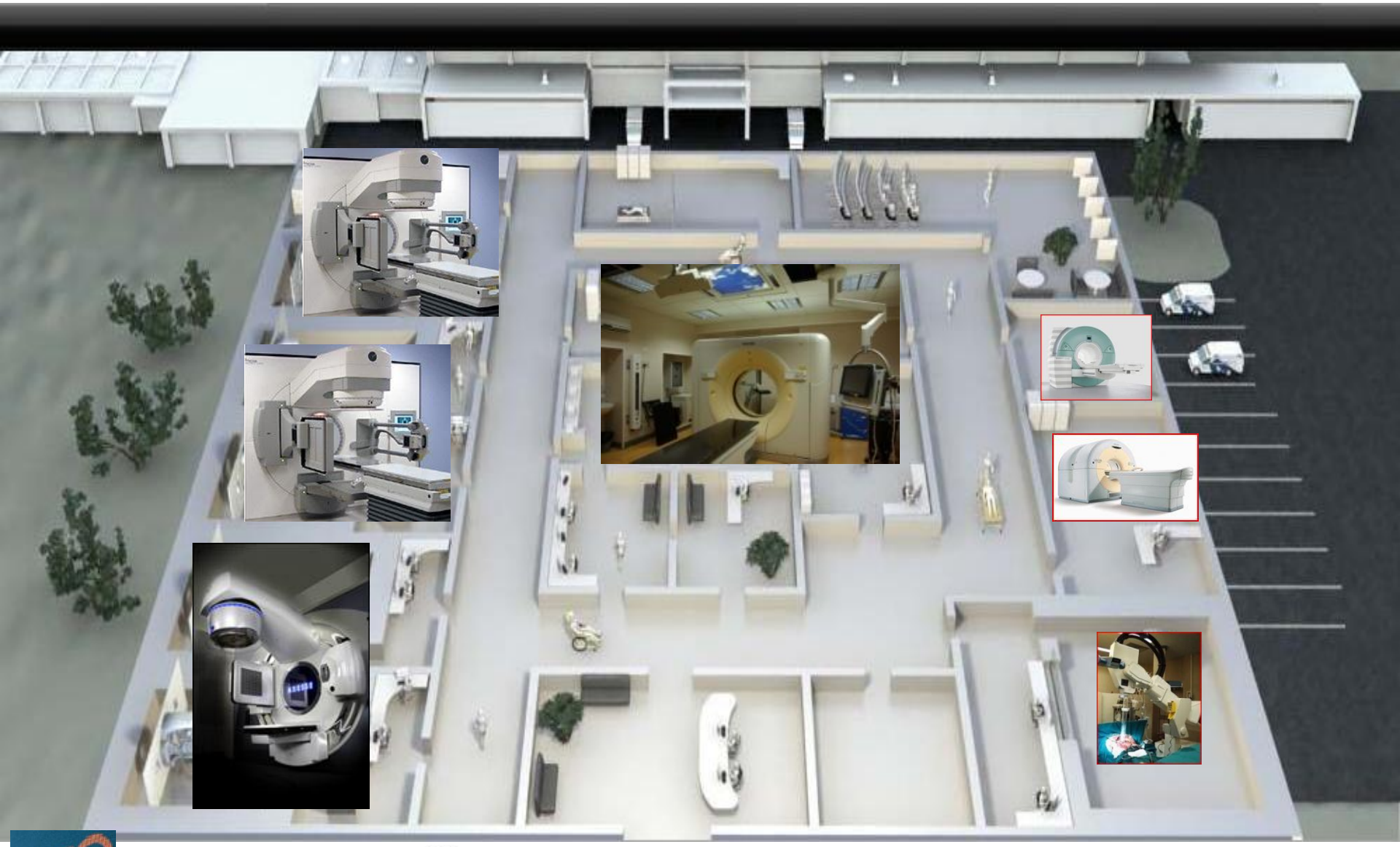

MasterPlan

ELEKTA MOSAIQ

ELEKTA MONACO

ELEKTA ERGO++

AAPM REPORT NO. 91

The Management of Respiratory Motion in Radiation Oncology

Report of AAPM Task Group 76

Members:

Paul J. Keall	Virginia Commonwealth University (Co-Chair)
Gig S. Mageras	Memorial Sloan-Kettering Cancer Center (Co-Chair)
James M. Balter	University of Michigan
Richard S. Emery	Saint Vincent's Cancer Center
Kenneth M. Forster	UT Southwestern Medical Center
Steve B. Jiang	Massachusetts General Hospital
Jeffrey M. Kapatoes	TomoTherapy, Inc.
Hideo D. Kubo	UC Davis Cancer Center (Deceased)
Daniel A. Low	Washington University
Martin J. Murphy	Virginia Commonwealth University
Brad R. Murray	Cross Cancer Institute
Chester R. Ramsey	Thompson Cancer Survival Center
Marcel B. van Herk	The Netherlands Cancer Institute
S. Sastry Vedam	UT M.D. Anderson Cancer Center
John W. Wong	Johns Hopkins University
Ellen Yorke	Memorial Sloan-Kettering Cancer Center

4DCT OUTLINE

- **Why is 4D CT necessary?**
- **What is 4D CT ?**
- **How do we characterize breathing ?**
- **What do we do with 4D information ?**

4th Dimension

Four-dimensional (4D) radiotherapy started to emerge in the early 2000s. An American Society of Radiation Oncology (ASTRO) panel on *Time: the* 4th *Dimension in Radiotherapy* at the 2003 annual meeting defined 4D radiotherapy as "the explicit inclusion of the temporal changes during the imaging, planning and delivery of radiotherapy". The definitions were further refined as: [35]

- **4D thoracic computed tomography (CT) imaging**: The acquisition of a sequence of CT image sets over consecutive segments of a breathing cycle

- **4D treatment planning**: Designing treatment plans on CT image sets obtained for each segment of the breathing cycle
- **4D treatment delivery**: Continuous delivery of the designed 4D treatment plan throughout the entire breathing cycle

4D CT imaging – Why?

Due to patient motion, such as respiratory, cardiac, digestive, and muscular motion, 3D imaging often produces images with **motion artifacts**.

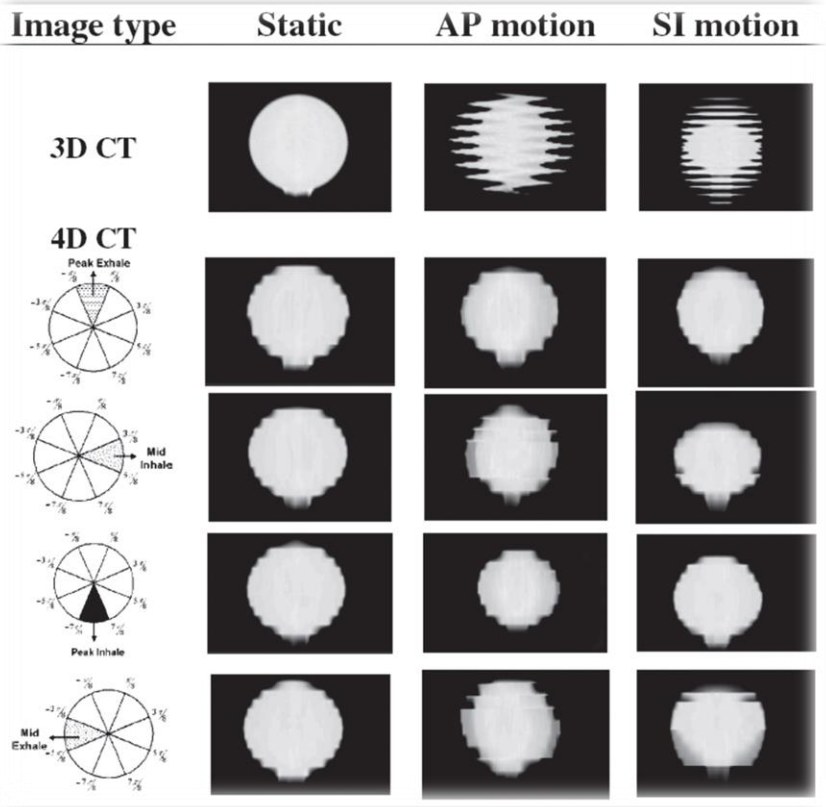

Guang Li et al.

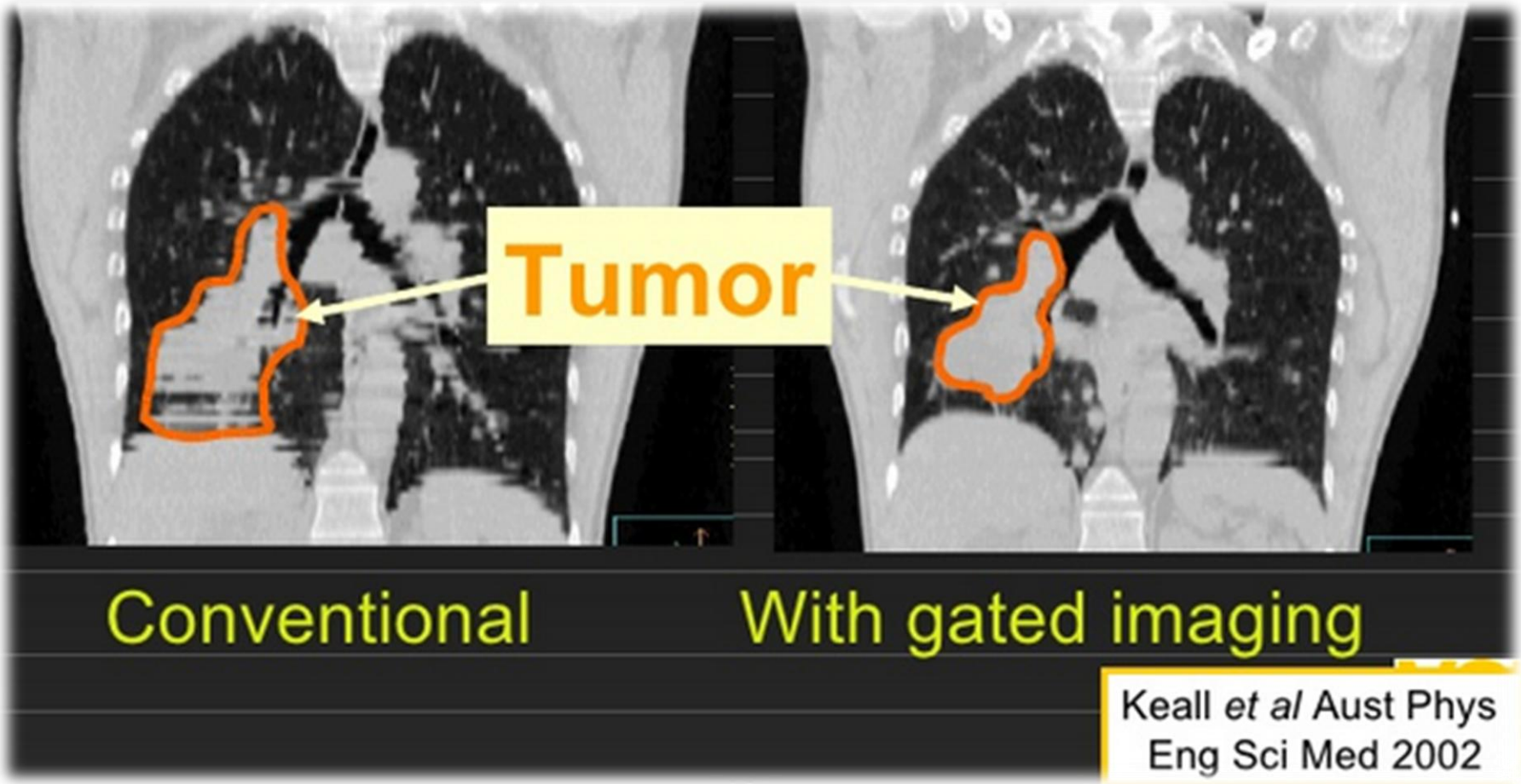
Tumor
Conventional
With gated imaging
Keall *et al* Aust Phys Eng Sci Med 2002

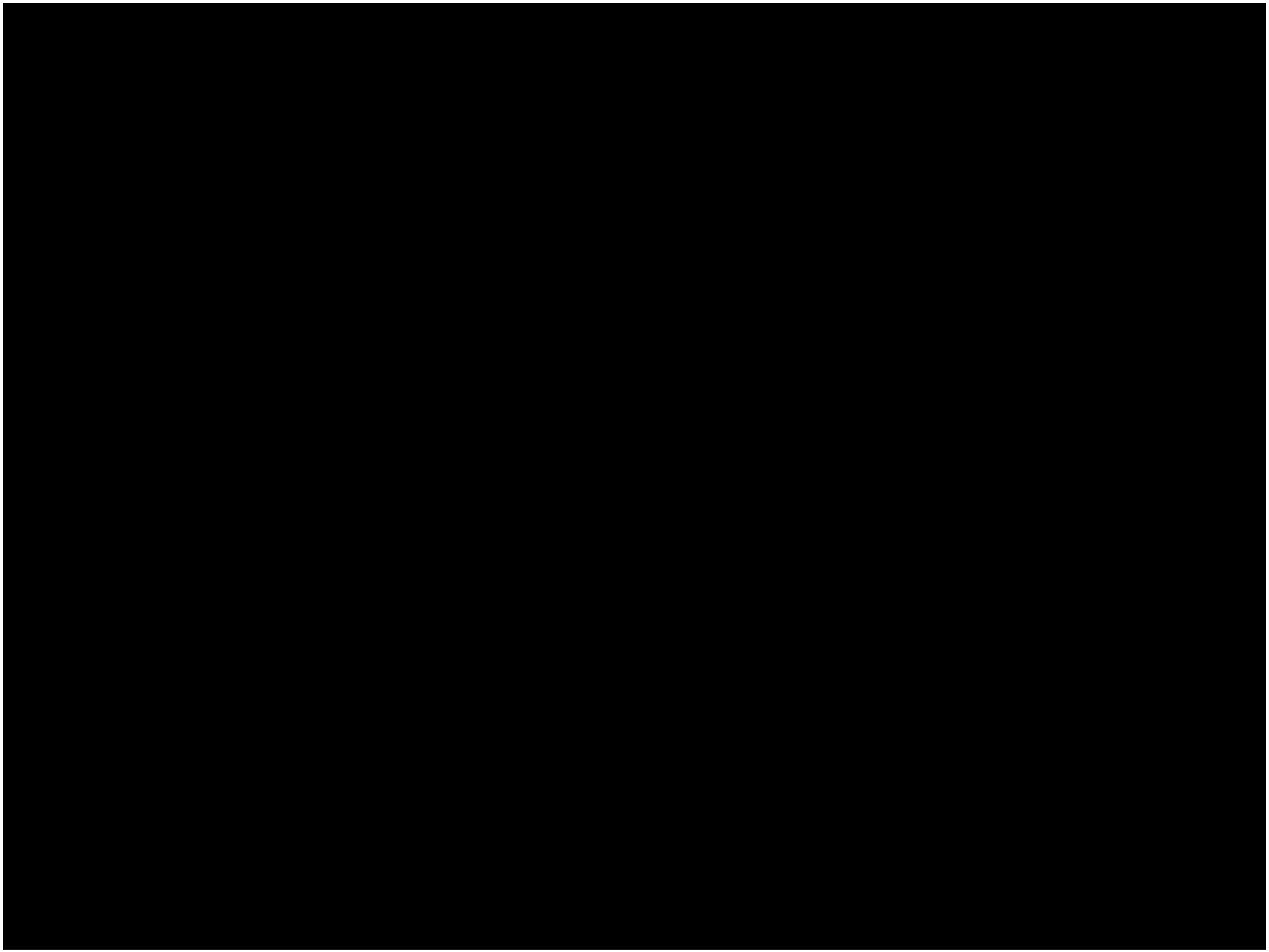

there are **no general patterns of respiratory behavior** that can be assumed for a particular patient prior to observation and treatment.

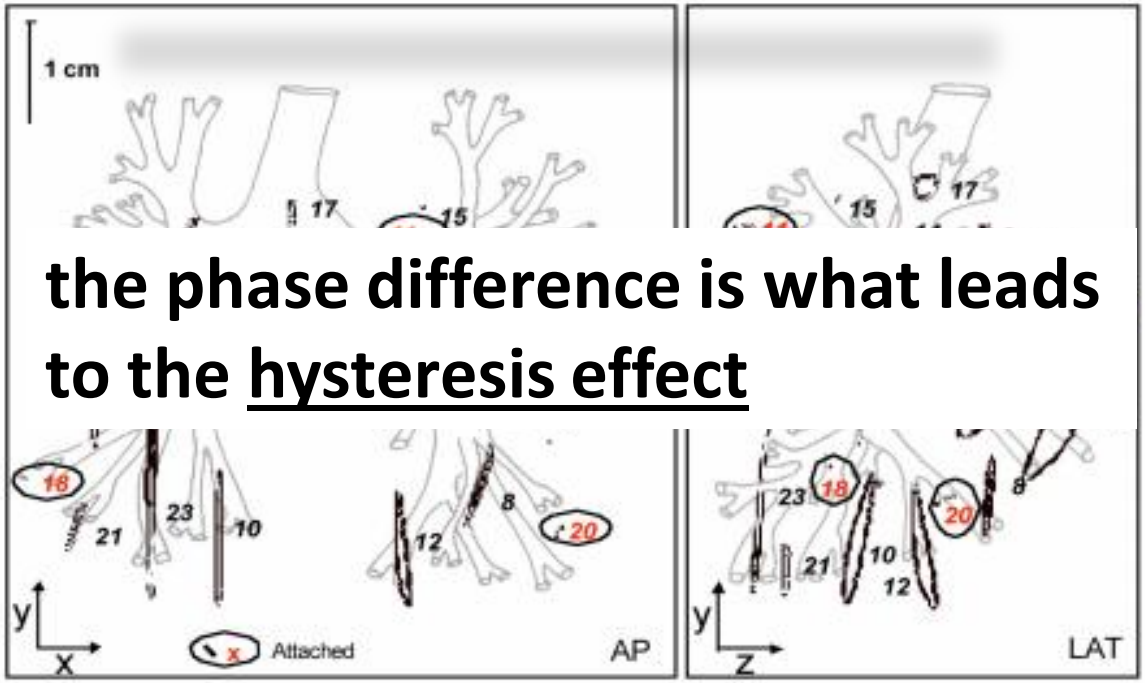

the phase difference is what leads to the hysteresis effect

Figure 5. Tumor trajectories (not to scale) in 23 lung tumor patients, measured using implanted markers and real-time stereoscopic fluoroscopy. [Reproduced from reference 67: *Int J Radiat Oncol Biol Phys*, vol 53, "Precise and real-time measurement of 3D tumor motion in lung due to breathing and heartbeat, measured during radiotherapy," Y. Seppenwoolde, H. Shirato, K. Kitamura, S. Shimizu, M. van Herk, J. V. Lebesque, and K. Miyasaka, pp. 822–834. © 2002, with permission from Elsevier.].

MID-VENTILATION CT SCAN CONSTRUCTION FROM FOUR-DIMENSIONAL RESPIRATION-CORRELATED CT SCANS FOR RADIOTHERAPY PLANNING OF LUNG CANCER PATIENTS

JOCHEM W. H. WOLTHAUS, M.SC., CHRISTOPH SCHNEIDER, PH.D., JAN-JAKOB SONKE, PH.D., MARCEL VAN HERK, PH.D., JOSÉ S. A. BELDERBOS, M.D., MADDALENA M. G. ROSSI, D.C.R.(R), R.T.T., JOOS V. LEBESQUE, M.D., PH.D., AND EUGÈNE M. F. DAMEN, PH.D.

Department of Radiation Oncology, The Netherlands Cancer Institute, Antoni van Leeuwenhoek Hospital, Amsterdam, The Netherlands

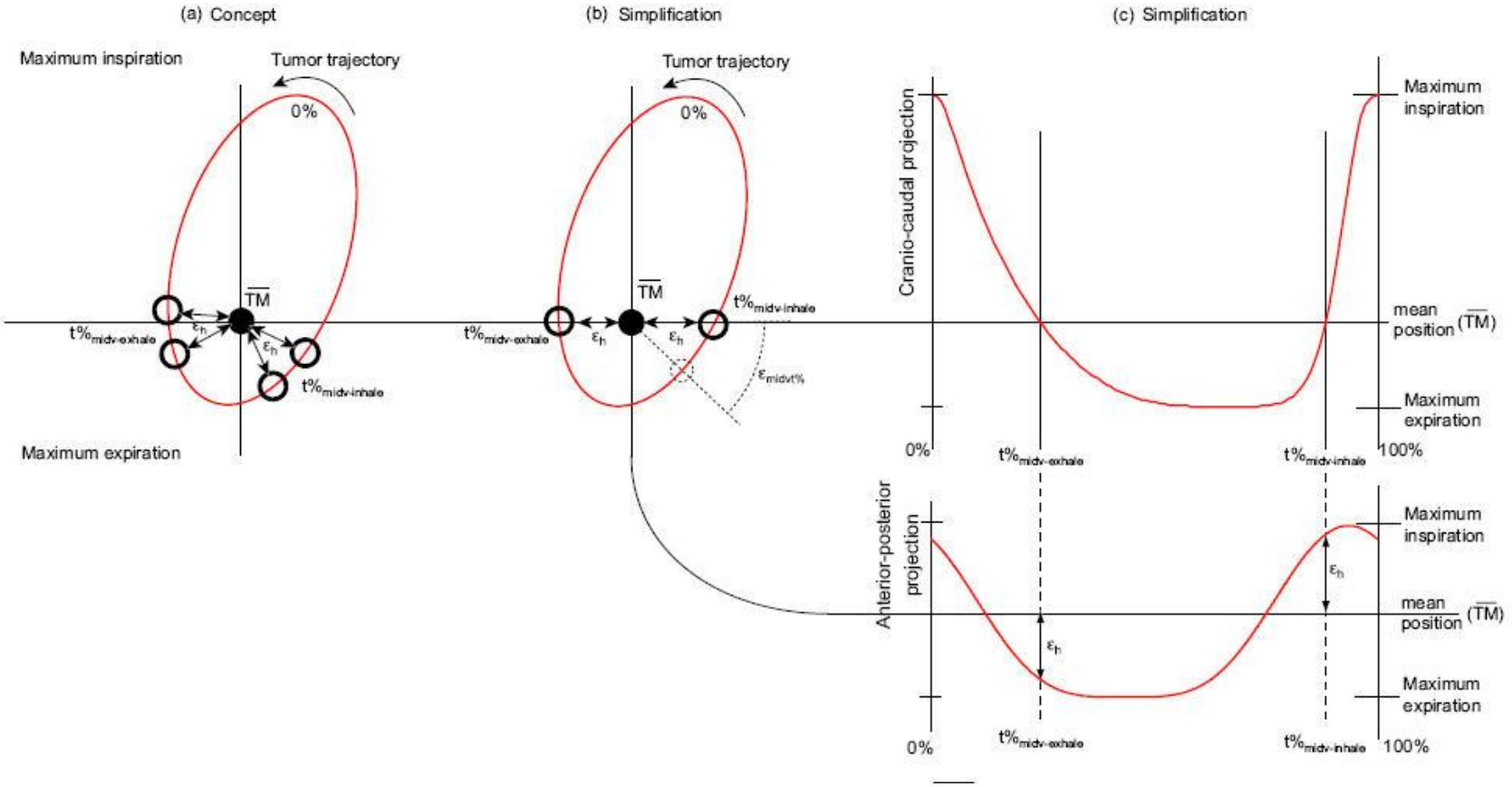

How to model this motion?

Passive Breathing tracking

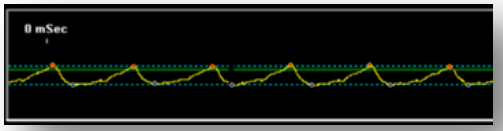

Breath holding & **Active** breathing control (ABC), visual coaching

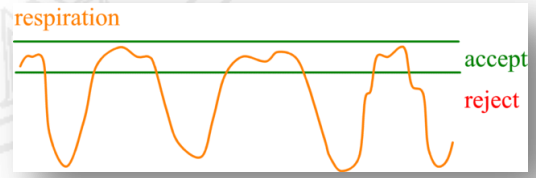

Respiratory gating

To perform any type of respiratory gating, it is obvious a ***device to monitor breathing*** is required

Philips bellows

Varian RPM.™

X. Li et al.

Sentinel

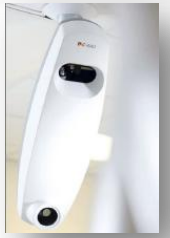

Pallotta et al.

Vision RT

If a **surrogate structure**, such as the chest wall or diaphragm, is used to signal tumor position for the purpose of beam gating or tracking, without observing the tumor directly during treatment, ***there will be uncertainties*** in the displacement and phase relationship between the surrogate and the tumor or other anatomy.

multiple driving forces in complex oscillatory mechanical system

These will be especially significant in the lung, where the mechanical **coupling** between the tumor and the surrogate structure is often **weak**, resulting in complex relationships between the two, and the breathing forces from the chest and/or the diaphragm

4D-CT Imaging Process

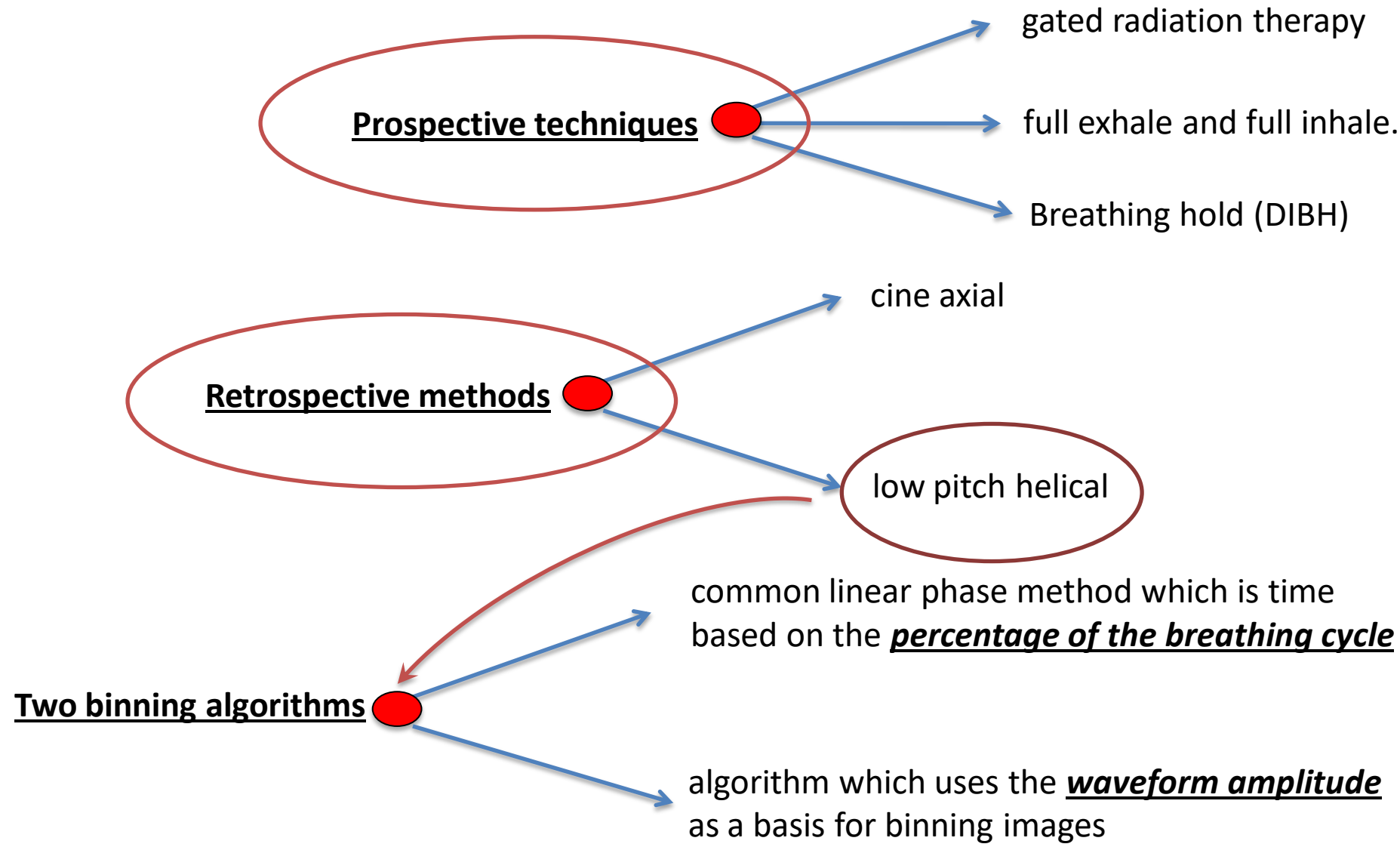

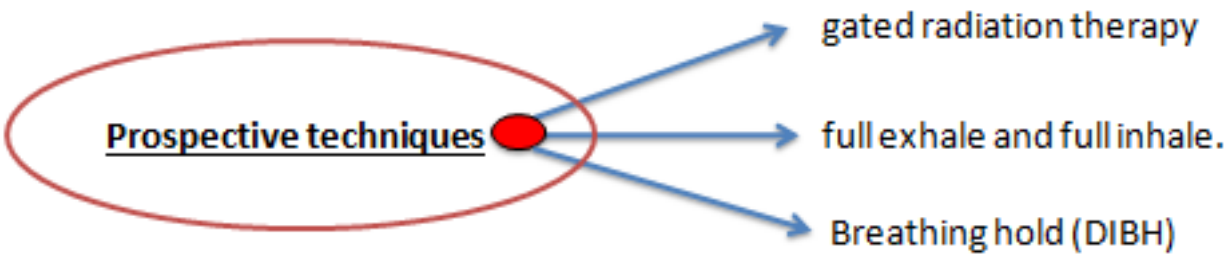

- ***axial***

is used to acquire a **single phase of the breathing Cycle** (a threshold can be set beyond the normal breathing range and allow the system to trigger on a large inhale or exhale

- ***spiral***

targeted **breathold** scanning protocol. In this procedure, the goal is to perform a rapid scan when the patient has reached a pre-determined respiratory threshold and ***maintains that level throughout the scan***.

Retrospective methods  low pitch helical

each voxel must remains illuminated by the CT X-rays for the entire breathing cycle

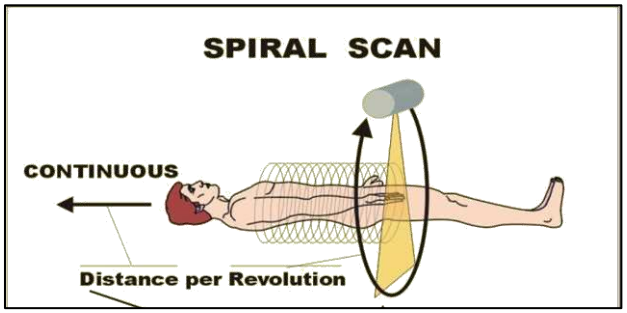

$$p_{max} = \left(\frac{t_{rot} \cdot f}{60}\right)\left(1 - \frac{FOV}{2R}\right)$$

***t*rot** *is the gantry rotation time*

f *is the patient's respiratory* ***frequency*** *(in breaths per minute)*

FOV *is the size of the reconstructed field of view (in mm)*

R *is the distance from the focus to the CT isocenter*

maximum scan time of **120 s** for Brillance Big Bore

$$v = \frac{p \cdot (N \times T)}{t_{rot}}$$

$$L_{max} = 120v - \Delta L$$

$$L_{max} = \frac{120p \cdot (N \times T)}{t_{rot}} - \Delta L$$

N × T is the detector collimation (in mm)

$$p_{max} = \left(\frac{t_{rot} \cdot f}{60}\right)\left(1 - \frac{FOV}{2R}\right)$$

$$L_{max} = 2f(N \times T)\left(1 - \frac{FOV}{2R}\right) - \Delta L$$

JOURNAL OF APPLIED CLINICAL MEDICAL PHYSICS, VOLUME 16, NUMBER 3, 2015

Helical 4D CT pitch management for the Brilliance CT Big Bore in clinical practice

Guido Hilgers,[a] Tonnis Nuver, André Minken
Department of Medical Physics, Radiotherapiegroep | Deventer, Deventer, The Netherlands
g.hilgers@radiotherapiegroep.nl

Received 30 May, 2014; accepted 21 December, 2014

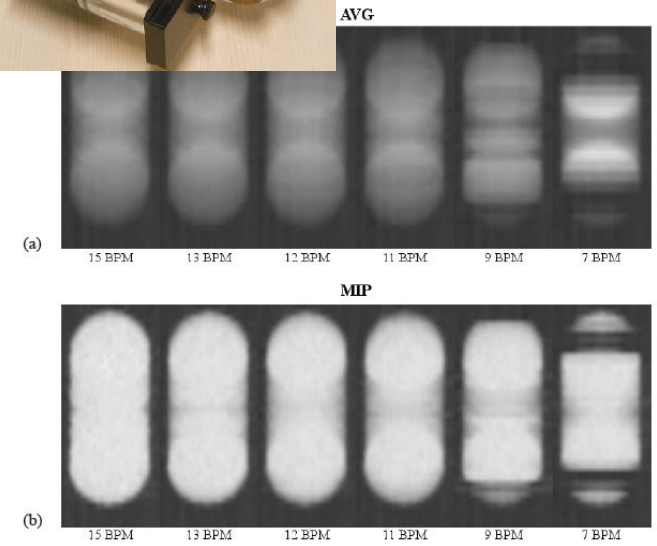

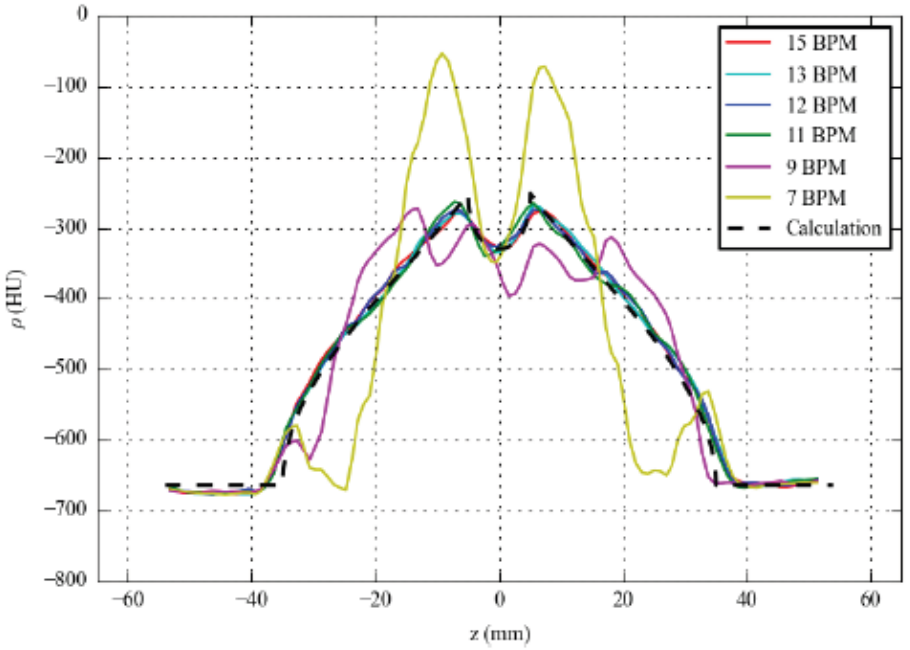

Two binning algorithms

Phase

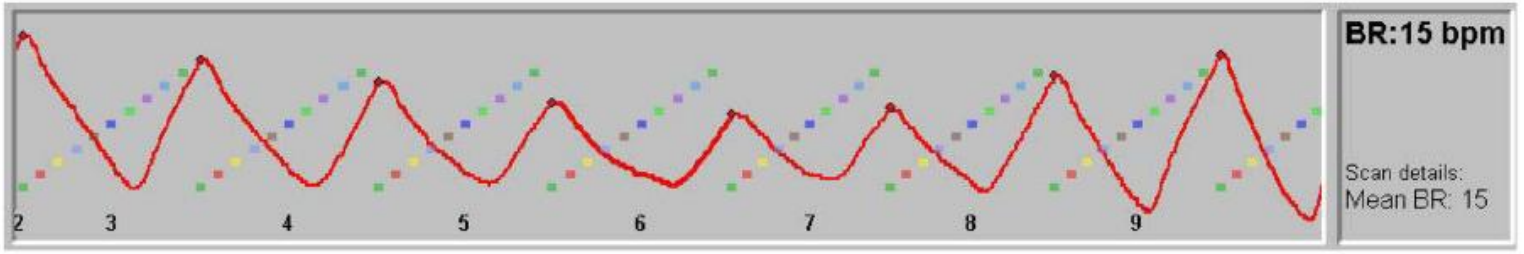

Amplitude

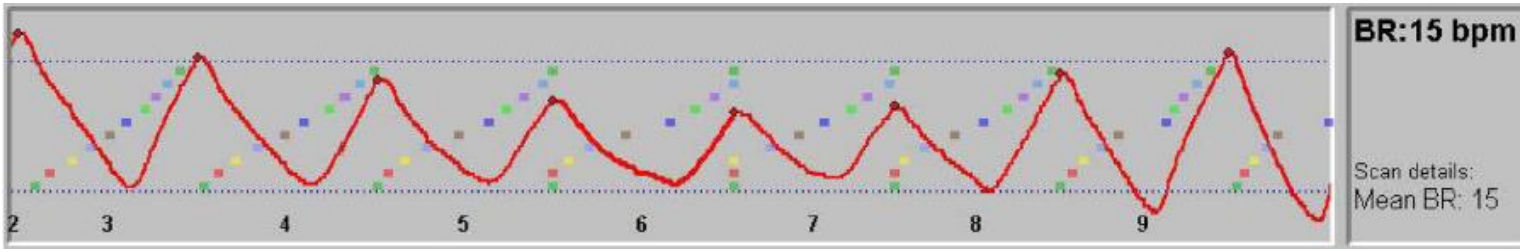

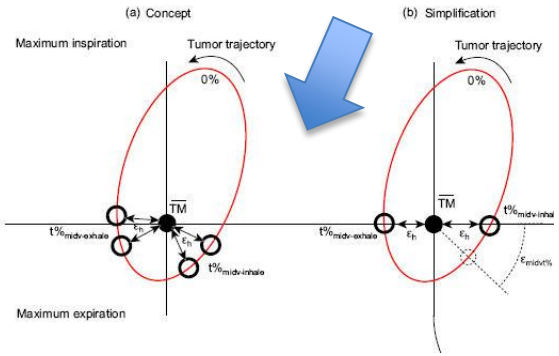

It is important to ***differentiate data collected during inhale vs. exhale.***

Phase **Amplitude**

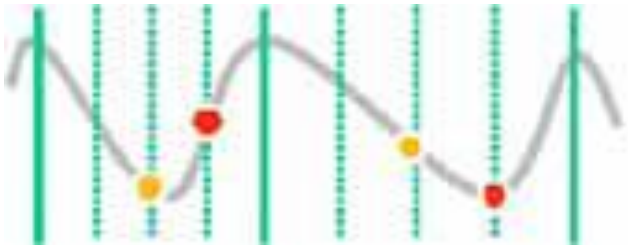

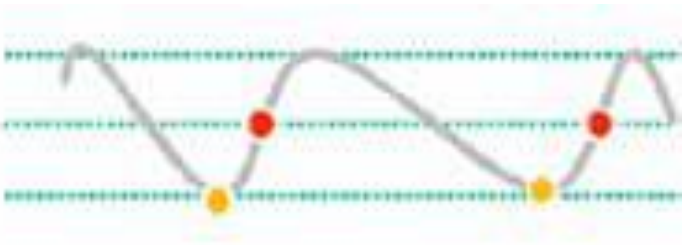

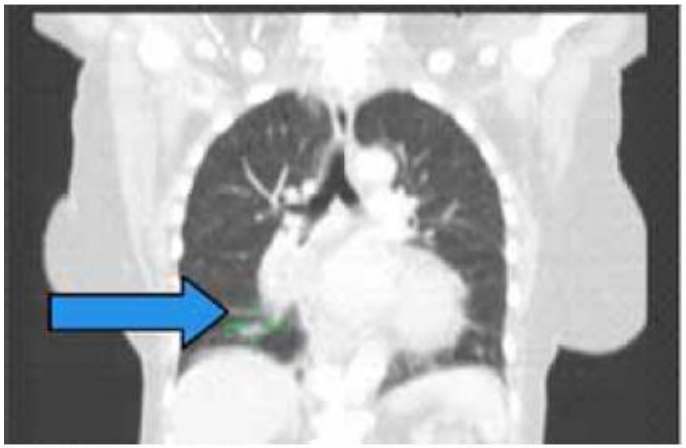

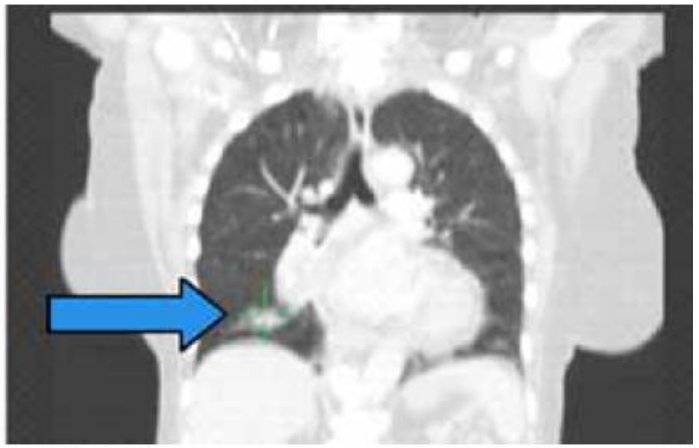

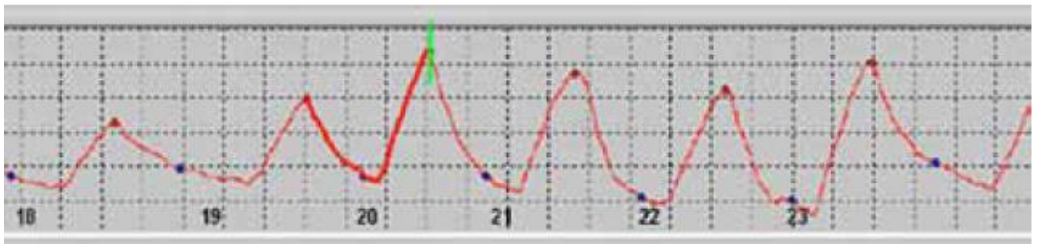

Clinical evaluations of an amplitude-based binning algorithm for 4DCT reconstruction in radiation therapy

Hua Li,[a] Camille Noel, and Jose Garcia-Ramirez
Department of Radiation Oncology, Washington University School of Medicine, St. Louis, Missouri 63110

Daniel Low
Department of Radiation Oncology, University of California Los Angeles, Los Angeles, California 90095

Jeffrey Bradley, Clifford Robinson, Sasa Mutic, and Parag Parikh
Department of Radiation Oncology, Washington University School of Medicine, St. Louis, Missouri 63110

Conclusions: Overall, the ***amplitude-binning algorithm for 4DCT reconstruction reduced the severity of tumor distortion and image artifacts*** compared to the phase-binning algorithm. However, the full range of motion may not be characterized using amplitude-binning algorithms. Despite superior performance***, amplitude binning can still be susceptible to motion artifacts caused by large variations in amplitude*** of respiratory waves.

Breathing statistics

useful to identify and classify the irregularities in the breathing waveform

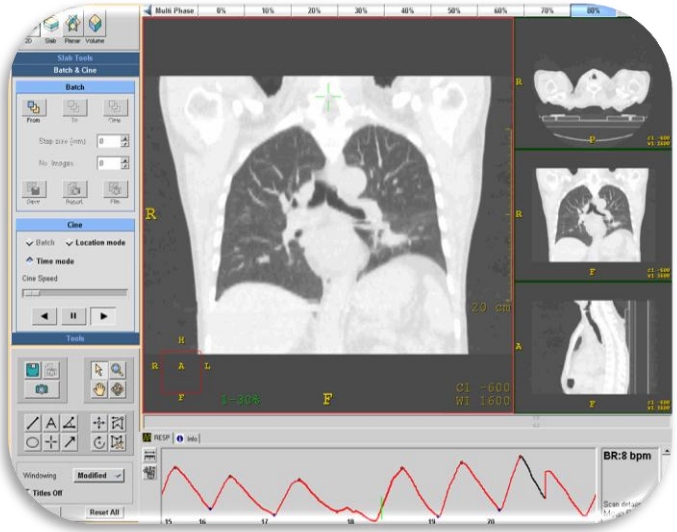

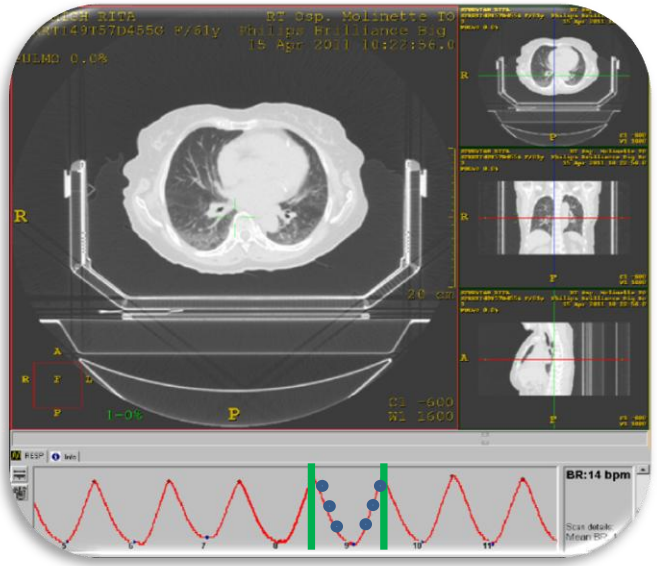

Scan lenght: 20	Average full exhalation phase: 58%
Numero di cicli catturati: 21	Average full inhalation phase: 99%
Mean BRT: 23 bpm	Amplitude range: 0.89-1.12
Breath rate range: 22-27 bpm	Amplitude standard deviation: 0.05

Breathing statistics

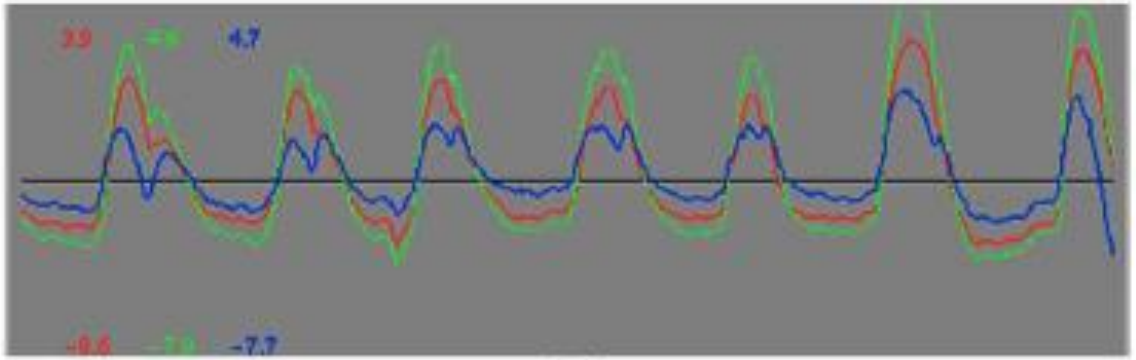

(a)

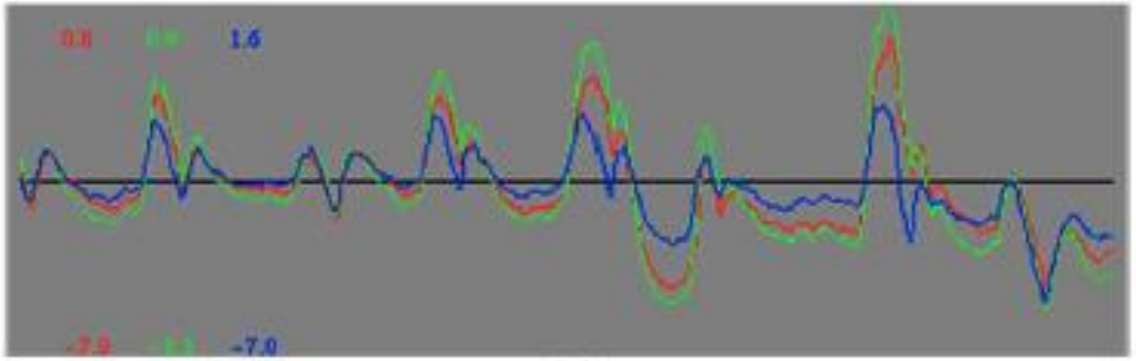

(b)

FIG. 2. Variations in respiratory patterns from the same patient taken a few minutes apart. The three curves in each plot correspond to infra-red reflector measured patient surface motion in the SI, AP, and ML directions, with each component arbitrarily normalized. In (a), the motion pattern is relatively reproducible in shape, displacement magnitude, and pattern. In (b), the trace is so irregular that it is difficult to distinguish any respiratory pattern. Figure courtesy of Dr. Sonja Dieterich.

QUALITY ASSURANCE OF 4D-CT SCAN TECHNIQUES IN MULTICENTER PHASE III TRIAL OF SURGERY VERSUS STEREOTACTIC RADIOTHERAPY (RADIOSURGERY OR SURGERY FOR OPERABLE EARLY STAGE (STAGE 1A) NON–SMALL-CELL LUNG CANCER [ROSEL] STUDY)

COEN W. HURKMANS, PH.D.,* MAARTEN VAN LIESHOUT, B.SC.,* DANNY SCHURING, PH.D.,*
MARIËLLE J. T. VAN HEUMEN, B.SC.,* JOHAN P. CUIJPERS, PH.D.,† FRANK J. LAGERWAARD, M.D., PH.D.,†
JOACHIM WIDDER, M.D., PH.D.,‡ UULKE A. VAN DER HEIDE, PH.D.,§ AND
SURESH SENAN, F.R.C.R., M.R.C.P., PH.D.†

$$z(t) = z_0 - R \times \cos^{2n}(\pi t/T - \phi)$$

Fig. 1. Quasar phantom.

Table 1. Computed tomography scanner and scan protocol details

Institute	CT scanner	Bins (*n*), type	Reconstruction for T = 3 and T = 6 (half beam or full beam)	Shortest rotation time (s)	Gantry rotation (s) and pitch (-) Stationary	Gantry rotation (s) and pitch (-) T = 3 (maximal DSC pitch)	Gantry rotation (s) and pitch (-) T = 6 (maximal DSC pitch)
1	Philips Brilliance BIG Bore	10-phase	Half + half	0.44	1/0.67	0.5/0.081 (0.15)	0.5/0.081 (0.079)
2	GE Lightspeed	10-phase	Half + full	0.5	0.5/1.3	0.5 / [4 s, 0.3 s]* (3.33)	0.6/[7 s, 0.6 s]* (6.5)
3	Siemens Biograph 40 PET-CT	8-amplitude	Half + half	0.33†	1/1.2	1/0.1 (0.27)	1/0.1 (0.15)
4	GE Lightspeed RT	20-phase	Full + full	1	1/0.75	1/[3.4, 0.15 s]* (4)	1/[7 s, 0.3 s]* (7)
5	Siemens Sensation Open	6-amplitude	Half + half	0.33†	0.5/0.5	0.5/0.1 (0.15)	1/0.1 (0.15)
6	Siemens Sensation Open	10-phase	Half + half	0.33†	0.5/0.95	0.5/0.1 (0.15)	1/0.15 (0.15)
7	Philips Brilliance BIG Bore	10-phase	Half + half	0.44	0.5/0.938	0.5/0.081 (0.15)	0.75/0.081 (0.115)
8	Philips Brilliance BIG Bore	10-phase	Half + half	0.44	0.75/0.813	0.44/0.081 (0.13)	0.44/0.065 (0.07)
9	Siemens Sensation Open	12-amplitude	Half + half	0.33†	1/1.2	0.5/0.1 (0.15)	1/0.1 (0.15)

Abbreviations: CT = computed tomography; DSC = Data Sufficiency Condition; Maximum pitch enabling the reconstruction of a full breathing cycle.
* Cine-mode scanning: data between square brackets are cine duration and interval between cine images.
† Optional.

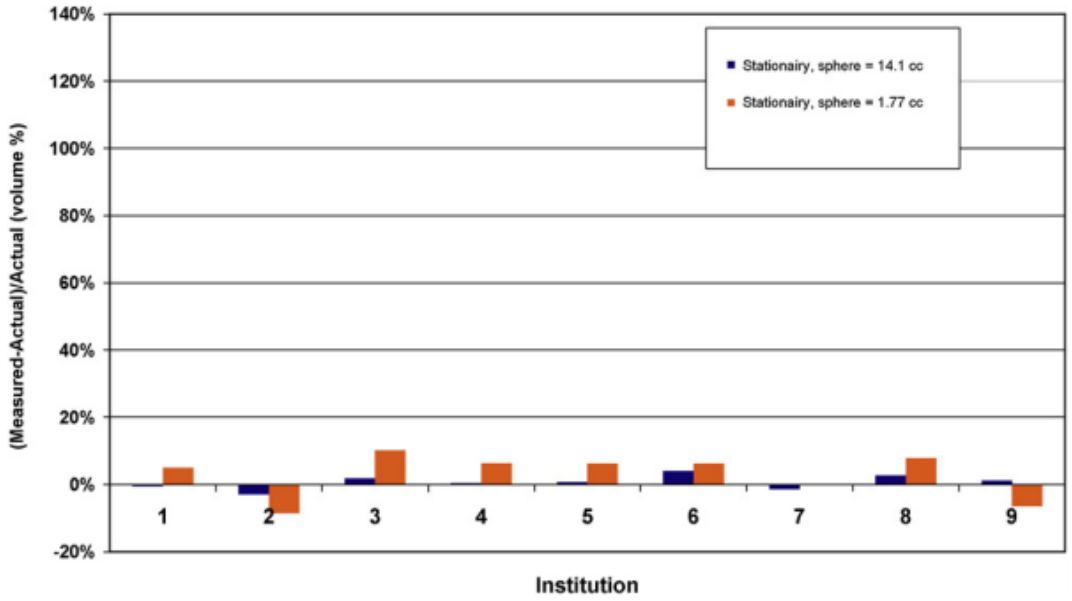

Fig. 4. Stationary volume deviations for all scans and institutions.

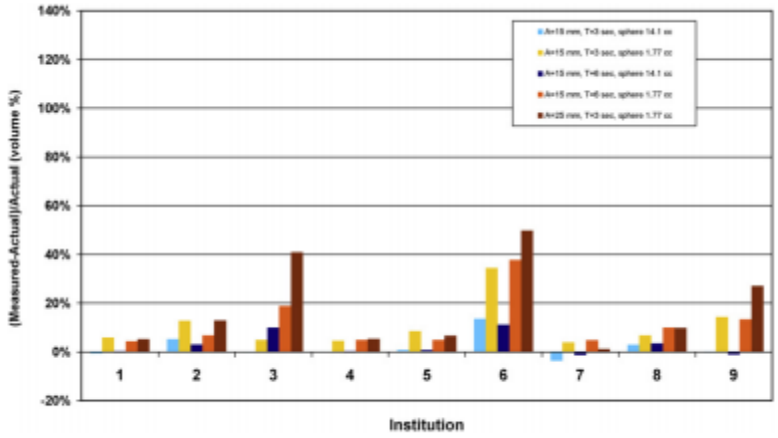

Fig. 5. End-expiration volume deviations for all scans and institutions. Same scaling used as in Fig. 4.

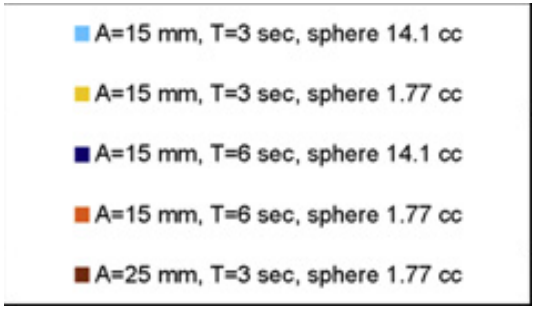

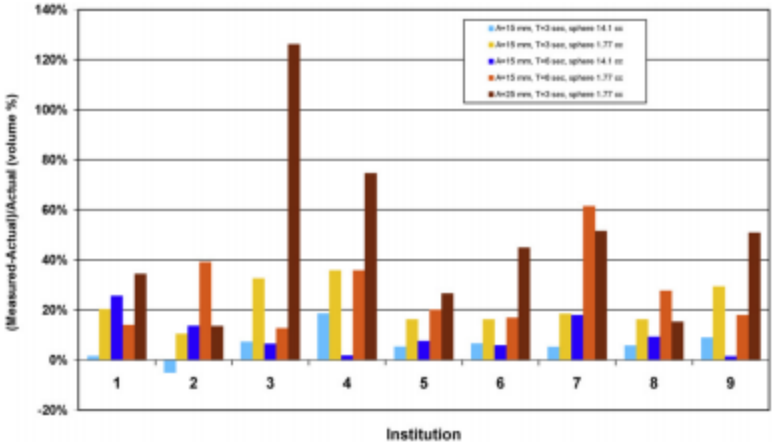

Fig. 7. Mid-ventilation volume deviation for all scans of moving phantom and all institutions. Same scaling used as in Fig. 4.

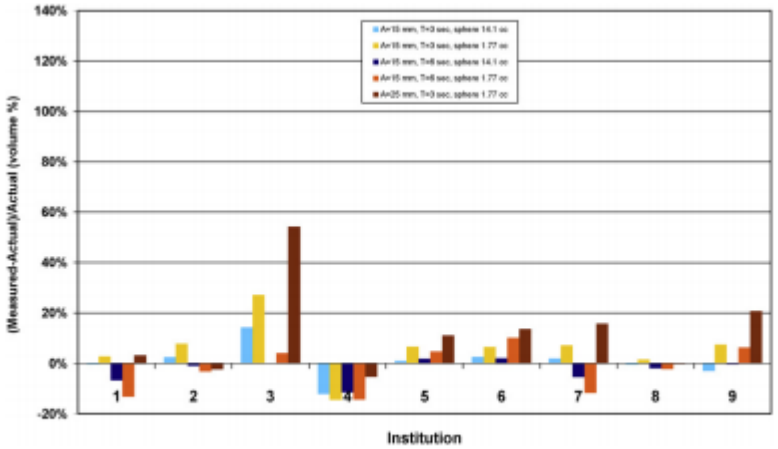

Fig. 8. Maximal intensity projection volume deviation for all scans of moving phantom and all institutions. Same scaling used as in Fig. 4.

Training

ACTIVE BREATHING CONTROL

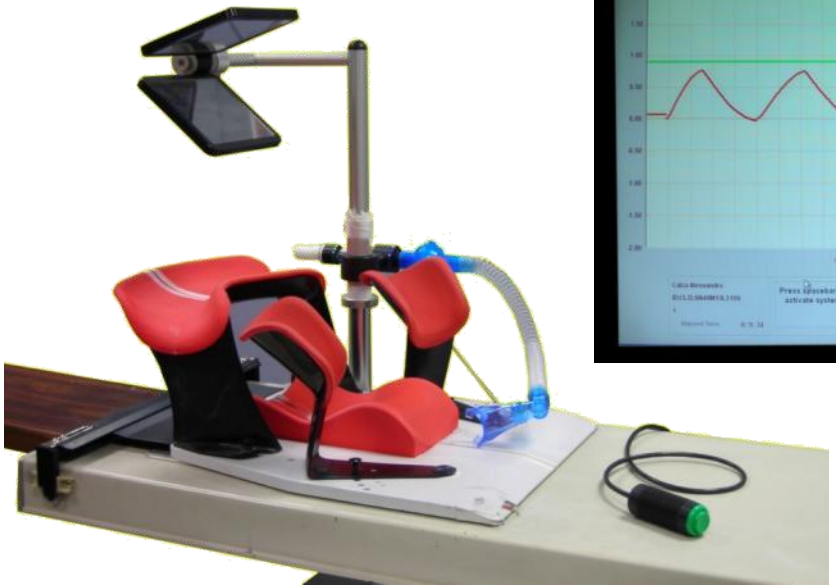

To reduce variability of respiratory movements

during the radiotherapy treatment

Training results

2 groups: Control group: 50 patients
Training group: 40 patients

A significantly higher proportion of patients in the training group had an acceptable amplitude variance (Fisher test p=0.03).

Poster #M4 : Breath training in lung SABR

What do we do with 4D information ?

MIP (Maximum Intensity Projection)
MinIP (Minimum Intensity Projection)
AVG (AverageProjection)

MIP

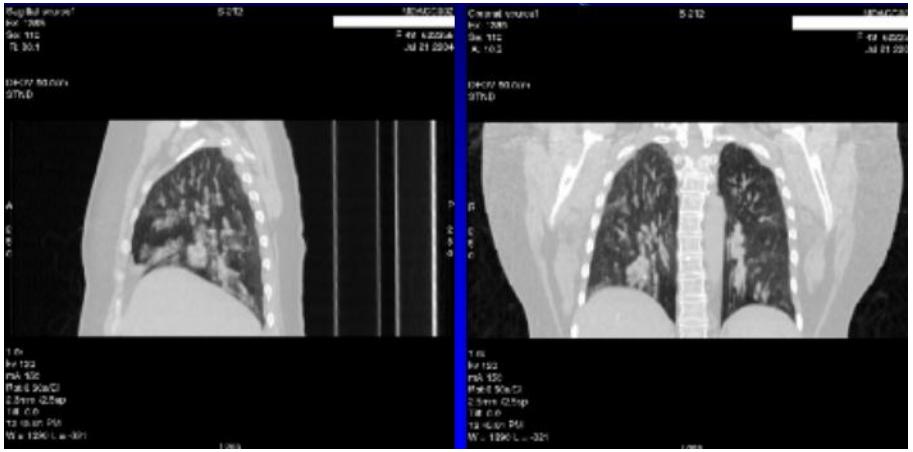

AVG

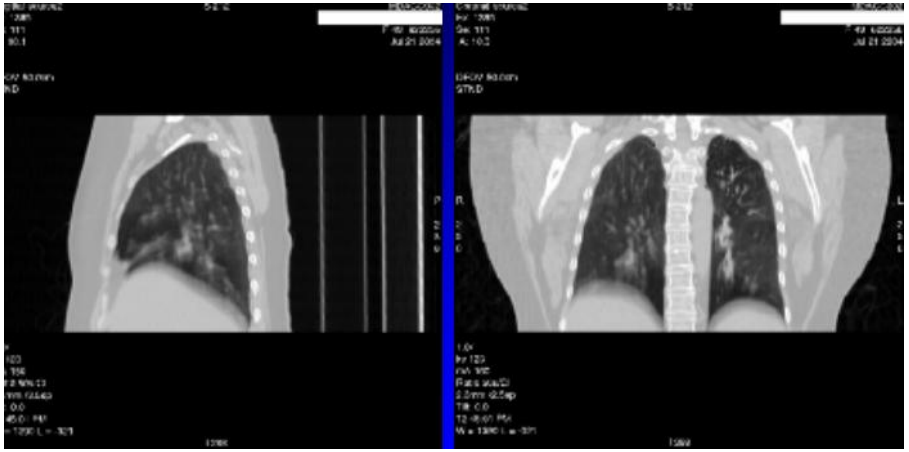

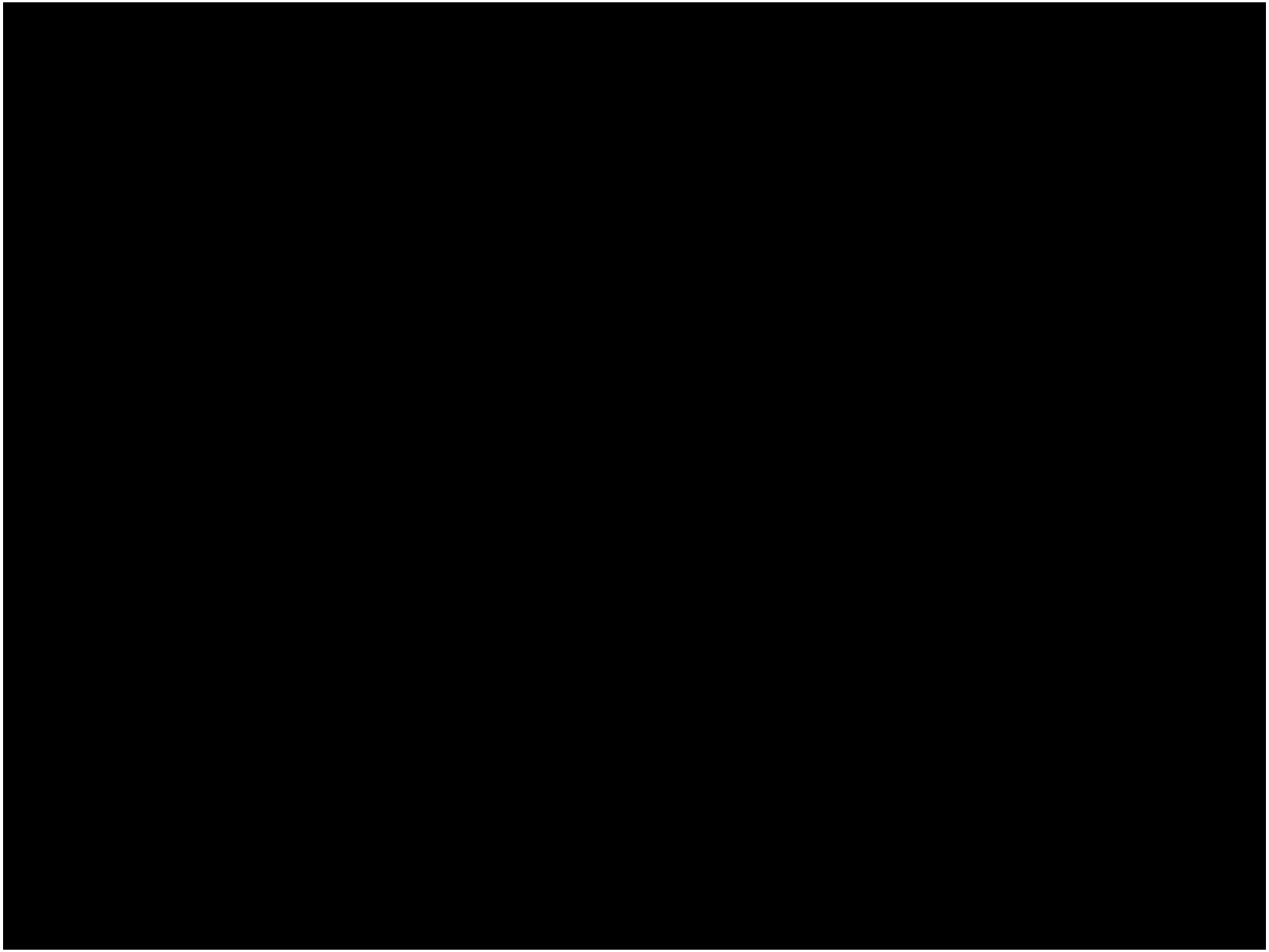

Comparison of helical, maximum intensity projection (MIP), and averaged intensity (AI) 4D CT imaging for stereotactic body radiation therapy (SBRT) planning in lung cancer

Jeffrey D. Bradley*, Ahmed N. Nofal, Issam M. El Naqa, Wei Lu, Jubei Liu, James Hubenschmidt, Daniel A. Low, Robert E. Drzymala, Divya Khullar

Department of Radiation Oncology, Washington University School of Medicine, St. Louis, MO, USA

MIP  (GTV)

PHYSICS CONTRIBUTION

COMPARISON OF DIFFERENT STRATEGIES TO USE FOUR-DIMENSIONAL COMPUTED TOMOGRAPHY IN TREATMENT PLANNING FOR LUNG CANCER PATIENTS

Jochem W. H. Wolthaus, M.Sc., Jan-Jakob Sonke, Ph.D., Marcel van Herk, Ph.D., José S. A. Belderbos, M.D., Ph.D., Maddalena M. G. Rossi, D.C.R. (R.), R.T.T., Joos V. Lebesque, M.D., Ph.D., and Eugène M. F. Damen, Ph.D.

Department of Radiation Oncology, The Netherlands Cancer Institute – Antoni van Leeuwenhoek Hospital, Amsterdam, The Netherlands

- Conventional
- ITV
- Mid-Position
- Gating (max inhale)

 (PTV)

Multimodal imaging platforms

Contents lists available at ScienceDirect

Radiotherapy and Oncology

journal homepage: www.thegreenjournal.com

PET in rectal cancer

The evaluation of a deformable image registration segmentation technique for semi-automating internal target volume (ITV) production from 4DCT images of lung stereotactic body radiotherapy (SBRT) patients

Richard Speight [a,*], Jonathan Sykes [a], Rebecca Lindsay [a], Kevin Franks [b], David Thwaites [a]

[a] Department of Medical Physics and Engineering; and [b] Department of Clinical Oncology, Leeds Teaching Hospitals Trust, Leeds, UK

DIR (ITV)

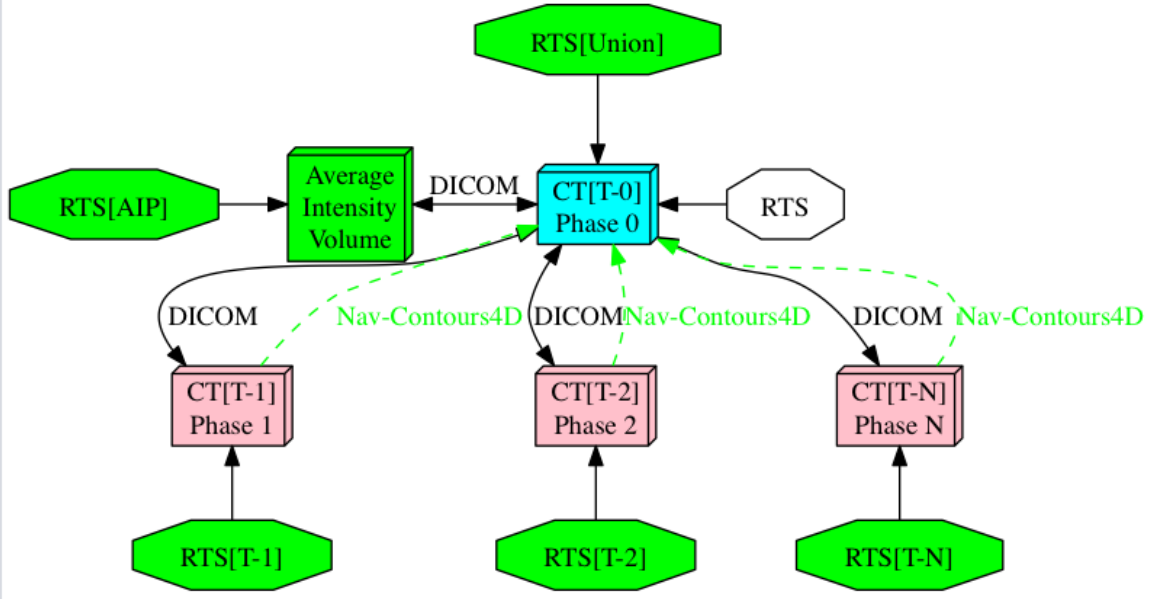

4DCT is an essential tool, but….

Uncertainties!!!

- Changes in respiratory patterns between simulation and treatment
- Tumor deformation from cycle to cycle and day to day
- Relationship between respiration signals and tumor motion and changes in this relationship throughout a course of radiotherapy
- Effects of **cardiac and gastrointestinal motion** on thoracic radiotherapy

- **Relationships between normal tissue and tumor motion**, particularly for normal tissue that is dose limiting and/or from which a useful motion signal (for imaging and treatment) can be obtained

Take home

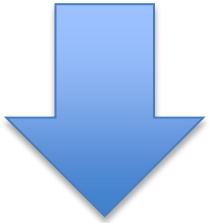

- Methods, such as **audiovisual feedback**, that can improve respiration reproducibility throughout the course of radiotherapy

Introduction to 4D-CBCT

when CBCT is applied **to thorax or upper abdomen regions**, the **image quality can be heavily degraded** due to patient respiratory motion

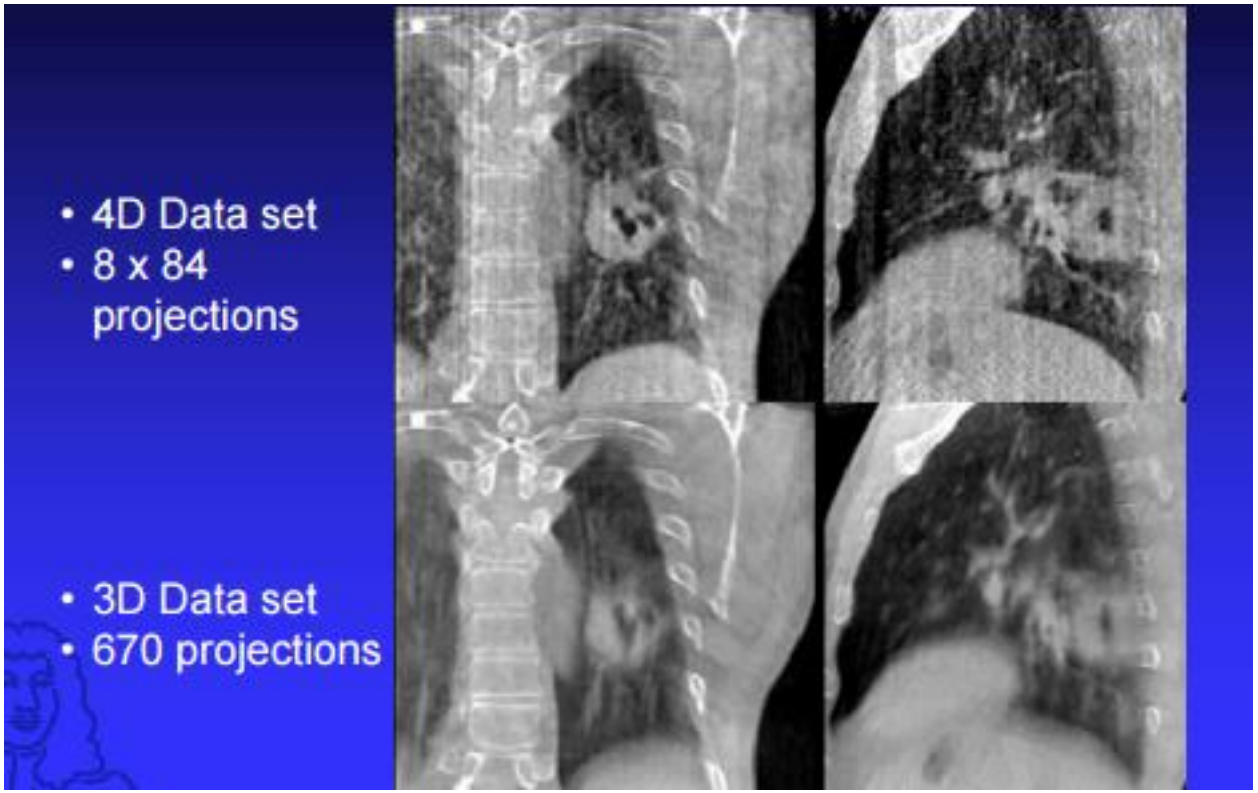

Courtesy of Sonke JJ

Introduction to 4D-CBCT

To overcome this problem, **four-dimensional CBCT** (4D-CBCT), or respiratory correlated CBCT has been developed to provide respiratory phase-resolved volumetric images for IGRT

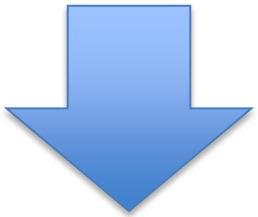

J. J. Sonke, L. Zijp, P. Remeijer, et al., "Respiratory correlated cone beam CT," Medical Physics 32, 1176-1186 (2005)

S. Kriminski, M. Mitschke, S. Sorensen, et al., "Respiratory correlated cone-beam computed tomography on an isocentric C-arm," Physics in Medicine and Biology 50, 5263-5280 (2005).

Li, L. Xing, P. Munro, et al., "Four-dimensional cone-beam computed tomography using an on-board imager," Medical Physics 33, 3825-3833 (2006).

L. Dietrich, S. Jetter, T. Tucking, et al., "Linac-integrated 4D cone beam CT: first experimental results," Physics in Medicine and Biology 51, 20 2939-2952 (2006).

J. Lu, T. M. Guerrero, P. Munro, et al., "Four-dimensional cone beam CT with adaptive gantry rotation and adaptive data sampling," Medical Physics 34, 3520-3529 (2007)

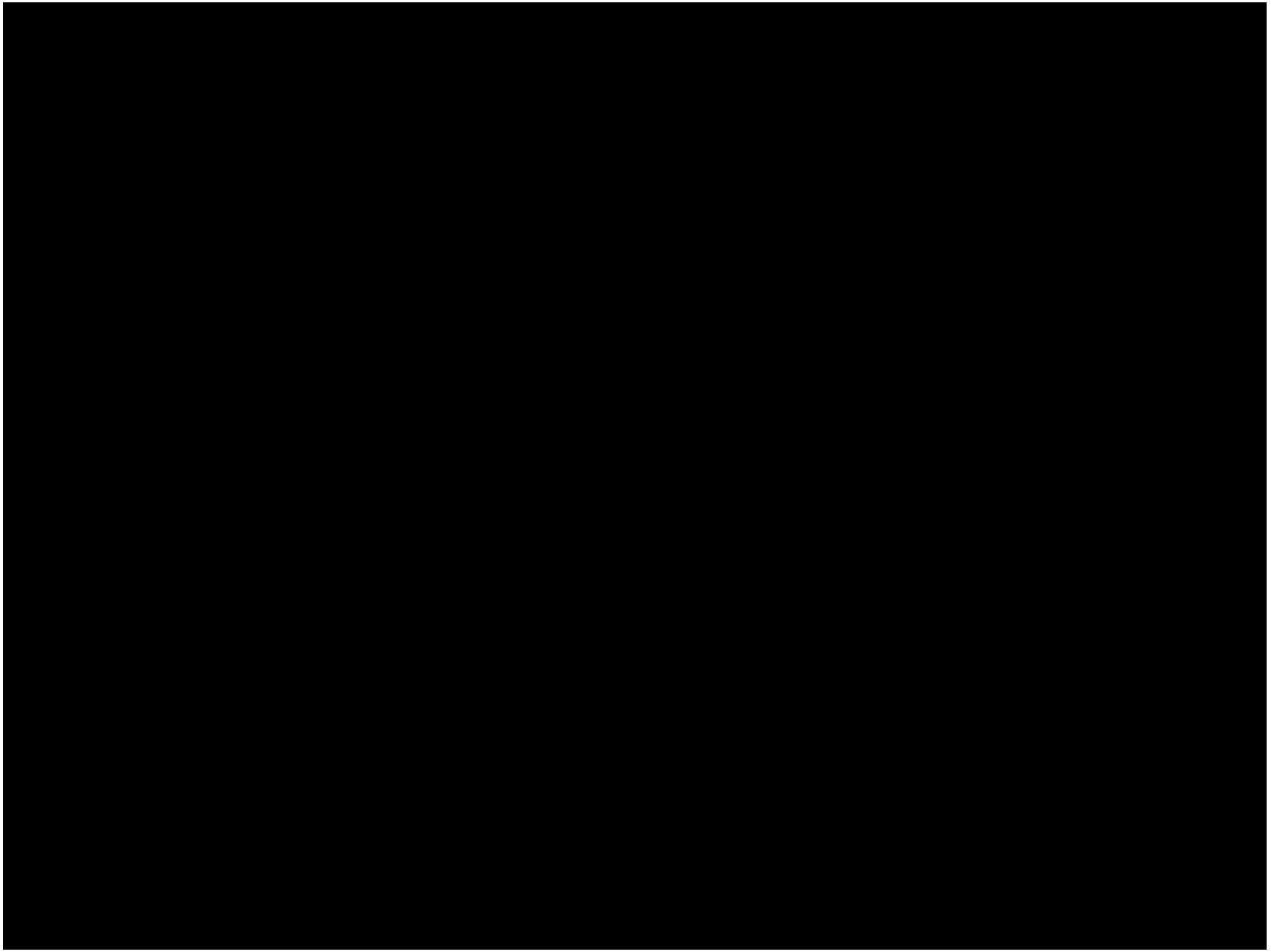

4D-CBCT

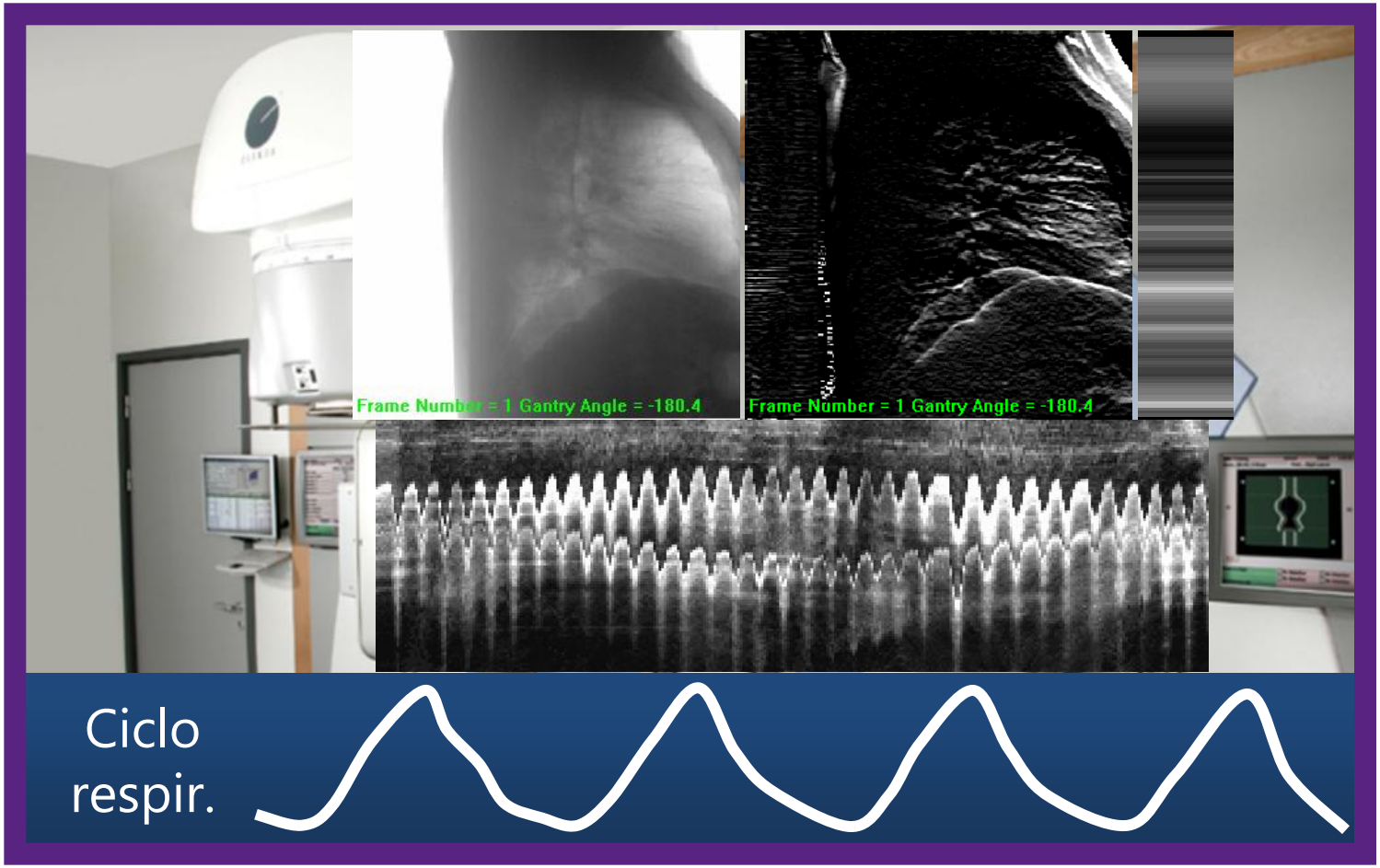
Frame Number = 1 Gantry Angle = -180.4
Frame Number = 1 Gantry Angle = -180.4
Ciclo respir.

4D-CBCT

4D-CBCT

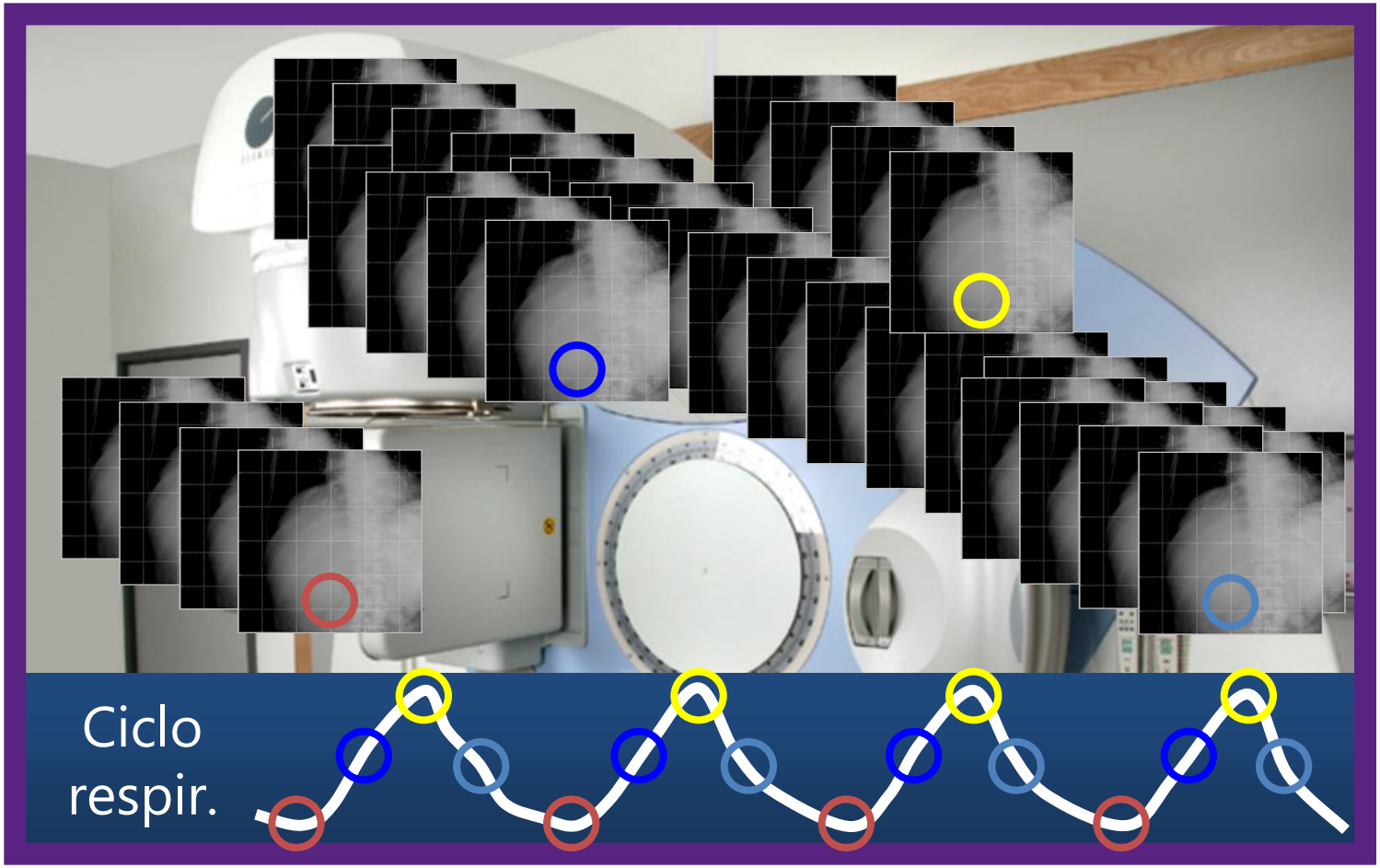

Respiratory correlated cone beam CT

Jan-Jakob Sonke,[a] Lambert Zijp, Peter Remeijer, and Marcel van Herk
Department of Radiation Oncology, The Netherlands Cancer Institute - Antoni van Leeuwenhoek Hospital, Plesmanlaan 121, 1066 CX Amsterdam, The Netherlands

(Received 27 May 2004; revised 12 January 2005; accepted for publication 12 January 2005; published 30 March 2005)

A cone beam computed tomography (CBCT) scanner integrated with a linear accelerator is a powerful tool for image guided radiotherapy. Respiratory motion, however, induces artifacts in CBCT, while the respiratory correlated procedures, developed to reduce motion artifacts in axial and helical CT are not suitable for such CBCT scanners. We have developed an alternative respiratory correlated procedure for CBCT and evaluated its performance. This respiratory correlated CBCT procedure consists of retrospective sorting in projection space, yielding subsets of projections that each corresponds to a certain breathing phase. Subsequently, these subsets are reconstructed into a four-dimensional (4D) CBCT dataset. The breathing signal, required for respiratory correlation, was directly extracted from the 2D projection data, removing the need for an additional respiratory monitor system. Due to the reduced number of projections per phase, the contrast-to-noise ratio in a 4D scan reduced by a factor 2.6–3.7 compared to a 3D scan based on all projections

Base line shift

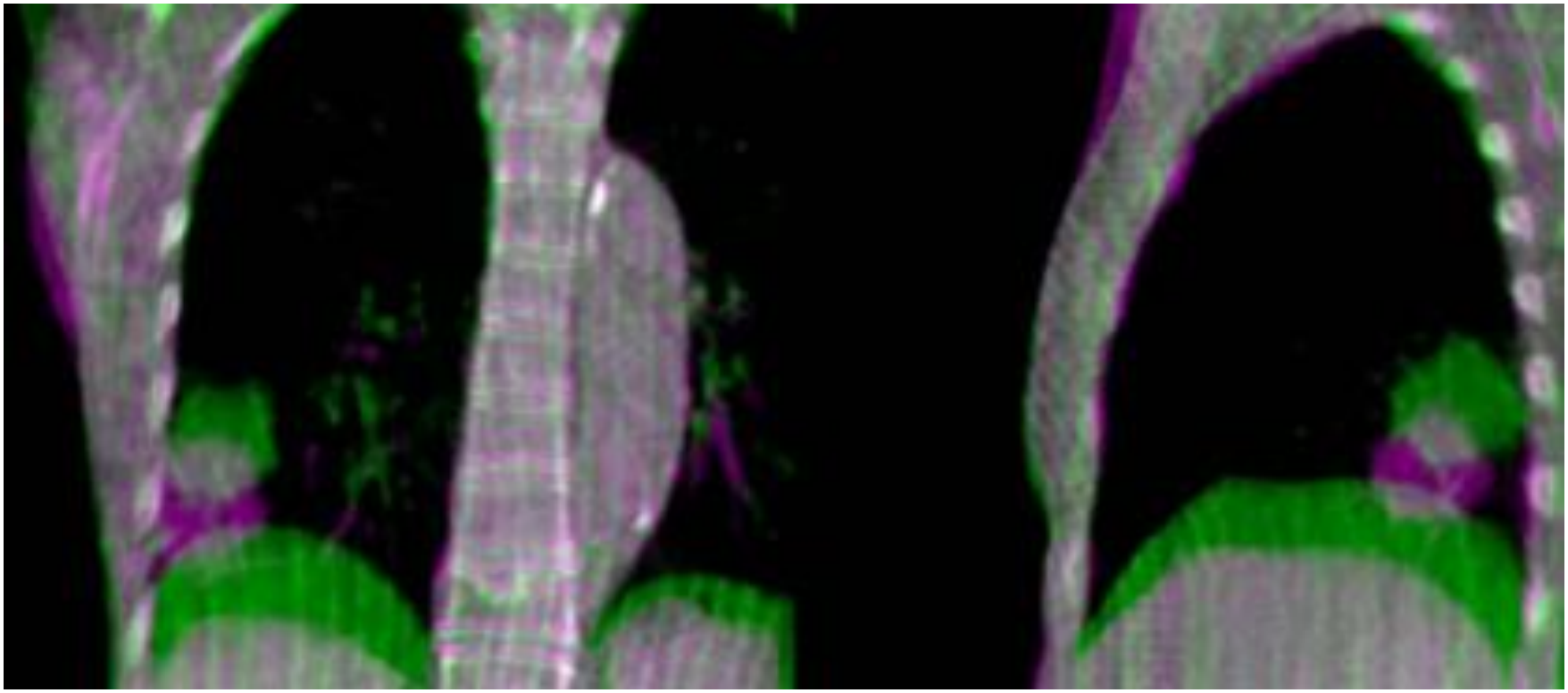

Tumor motion is very similar but occurs at very different places!!!

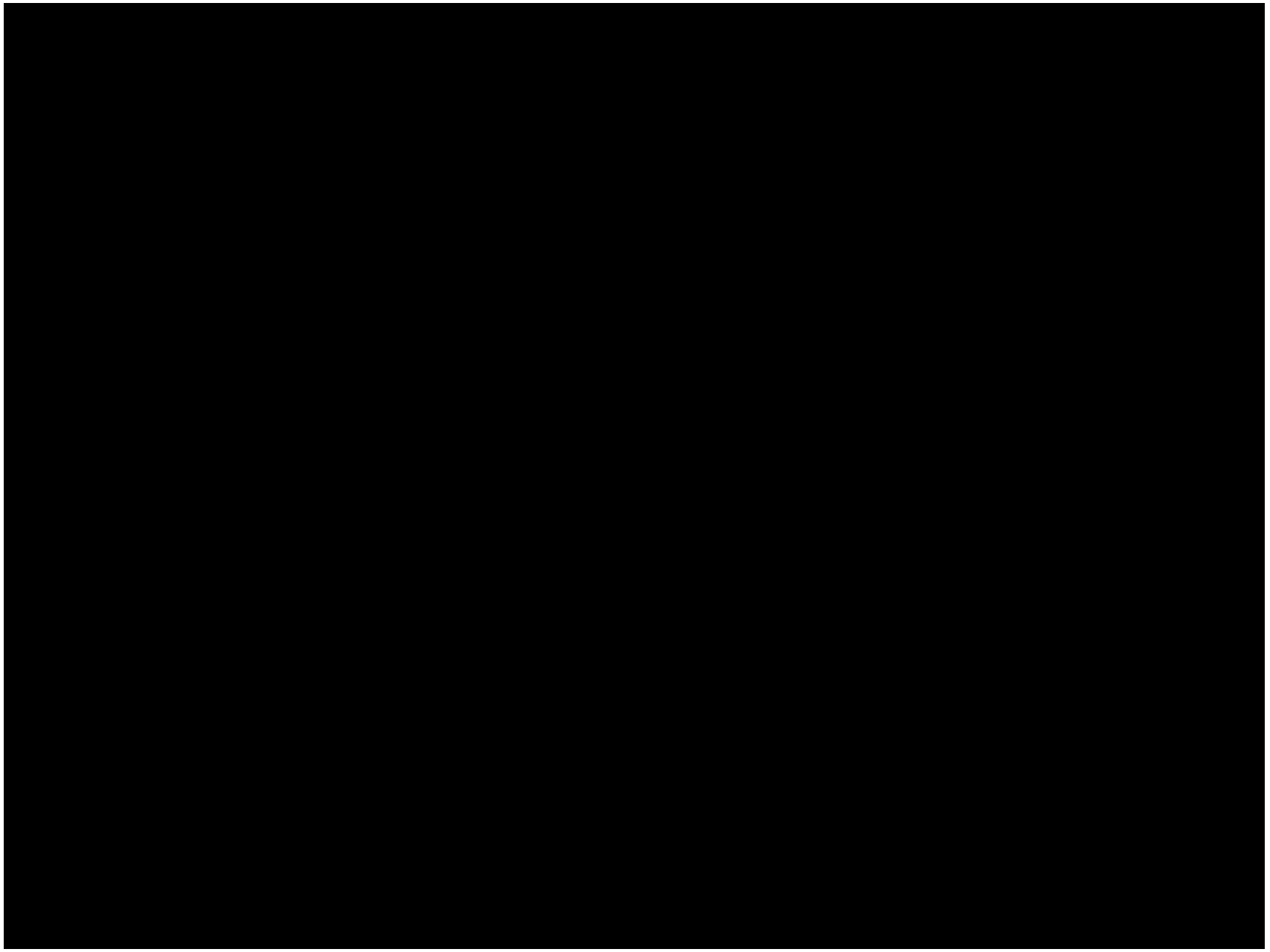

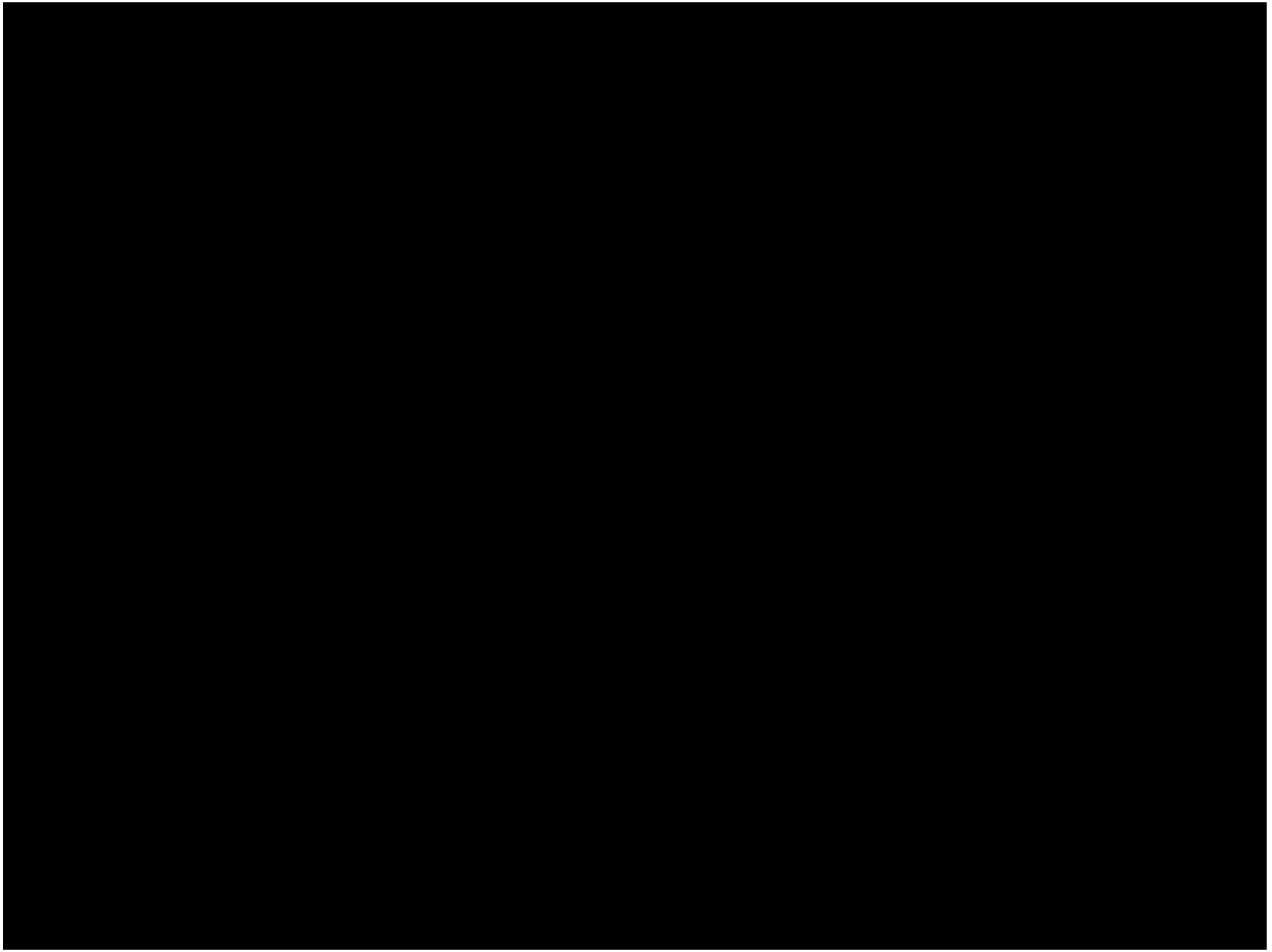

REFERENCES

1. Harsolia A, Hugo GD, Kestin LL, Grills IS, Yan D. Dosimetric advantages of four-dimensional adaptive image-guided radiotherapy for lung tumors using online cone-beam computed tomography. Int J Radiat Oncol Biol Phys. 2008;70(2):582–89.
2. Sonke JJ, Zijp L, Remeijer P, van Herk M. Respiratory correlated cone beam CT. Med Phys. 2005;32(4):1176–86.
3. Wolthaus W, Schneider C, Sonke JJ, et al. Mid-ventilation CT scan construction from four-dimensional respiration-correlated CT scans for radiotherapy planning of lung cancer patients. Int J Radiat Oncol Biol Phys. 2006;65(5):1560–71.
4. Clements N, Kron T, Franich R et al. The effect of irregular breathing patterns on internal target volumes in four-dimensional CT and cone-beam CT images in the context of stereotactic lung radiotherapy. Med Phys. 2013;40(2):021904.
5. Lu J, Guerrero TM, Munro P, et al. Four-dimensional cone beam CT with adaptive gantry rotation and adaptive data sampling. Med Phys. 2007;34(9):3520–29.
6. Elekta. Clinical user manual for XVI R4.5 general release. Crowley, UK: Elekta Ltd.; 2013.
7. Amer A, Marchant T, Sykes J, Czajka J, Moore C. Imaging doses from the Elekta Synergy X-ray cone beam CT system. Br J Radiol. 2007;80(954):476–82.
8. Feldkamp L, Davis L, Kress J. Practical cone-beam algorithm. JOSA A. 1984;1(6):612–19.
9. Dixon RL. A new look at CT dose measurement: beyond CTDI. Med Phys. 2003;30(6):1272–80.
10. Hyer DE and Hintenlang DE. Estimation of organ doses from kilovoltage cone-beam CT imaging used during radiotherapy patient position verification. Med Phys. 2010;37(9):4620–26.
11. Mori S, Endo M, Nishizawa K, et al. Enlarged longitudinal dose profiles in cone-beam CT and the need for modified dosimetry. Med Phys. 2005;32(4):1061–69.
12. AAPM. The measurement, reporting, and management of radiation dose in CT. AAPM Report No. 96. Report of AAPM Taks Group 23. College Park, MD: AAPM; 2008. Available from: https://www.aapm.org/pubs/reports/RPT_96.pdf
13. Lujan AE, Larsen EW, Balter JM, Ten Haken RK. A method for incorporating organ motion due to breathing into 3D dose calculations. Med Phys. 1999;26(5):715–20.
14. Ott JG, Becce F, Monnin P, Schmidt S, Bochud FO, Verdun FR. Update on the non-prewhitening model observer in computed tomography for the assessment of the adaptive statistical and model-based iterative reconstruction algorithms. Phys Med Biol. 2014;59(15):4047–64.

Lung SBRT : a flowchart for decision making from 4DCT to 4DCBCT

Contouring

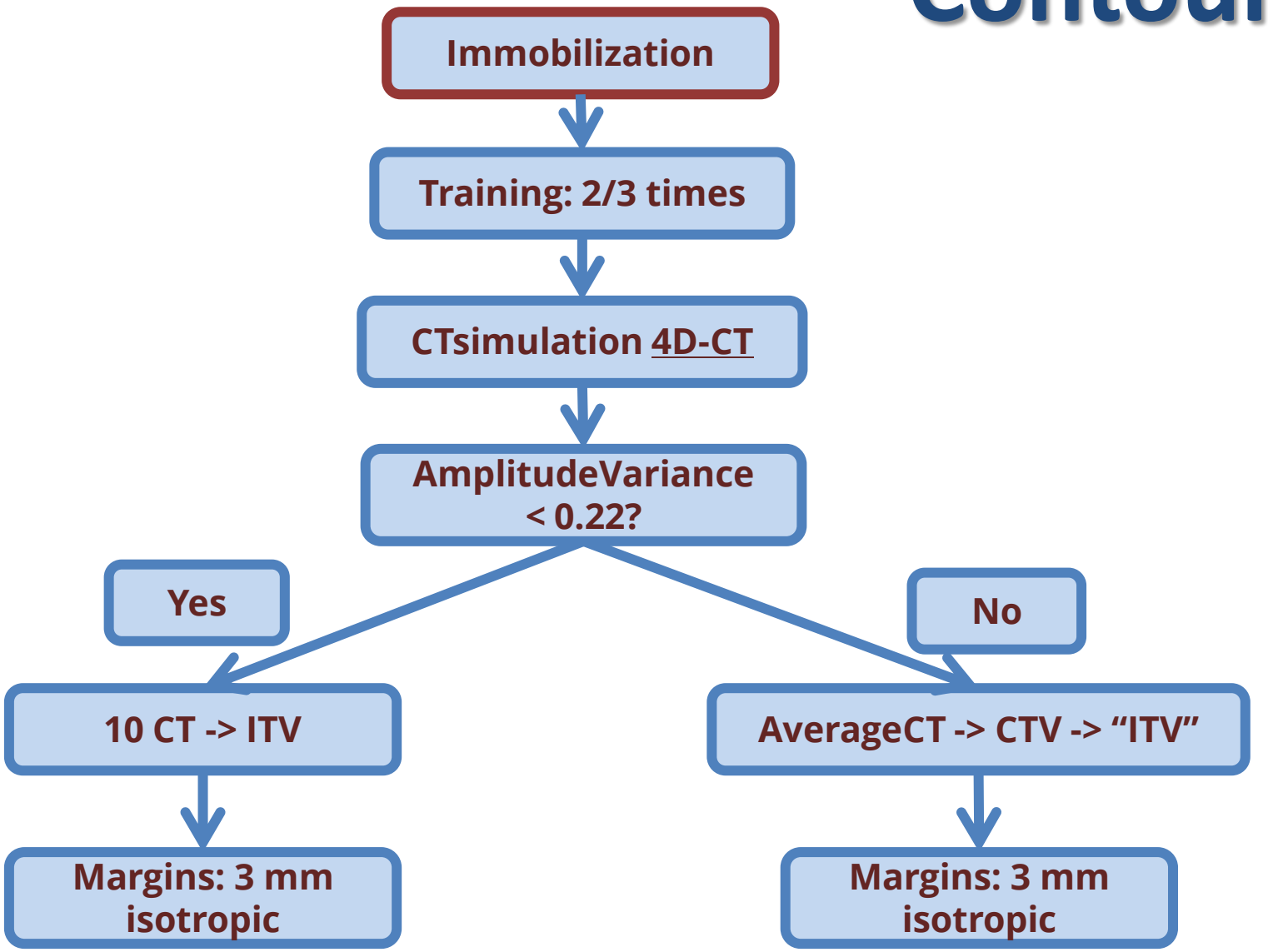
Immobilization
Training: 2/3 times
CTsimulation 4D-CT
AmplitudeVariance < 0.22?
Yes
No
10 CT -> ITV
AverageCT -> CTV -> "ITV"
Margins: 3 mm isotropic
Margins: 3 mm isotropic

Immobilization

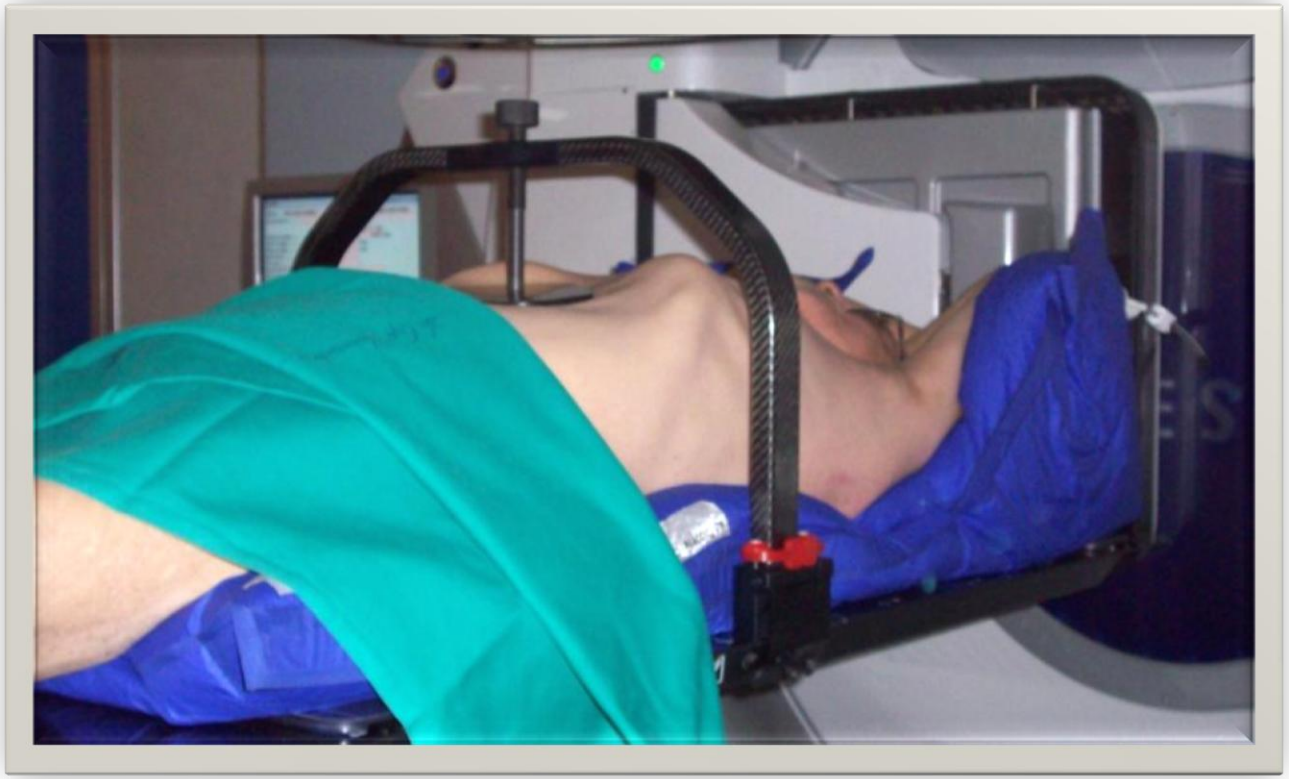

Vacuum immobilisation reduces tumour excursion and minimizes intrafraction error in a cohort study of stereotactic ablative body radiotherapy for pulmonary metastases (Shankar Siva et al 2014)

Contouring

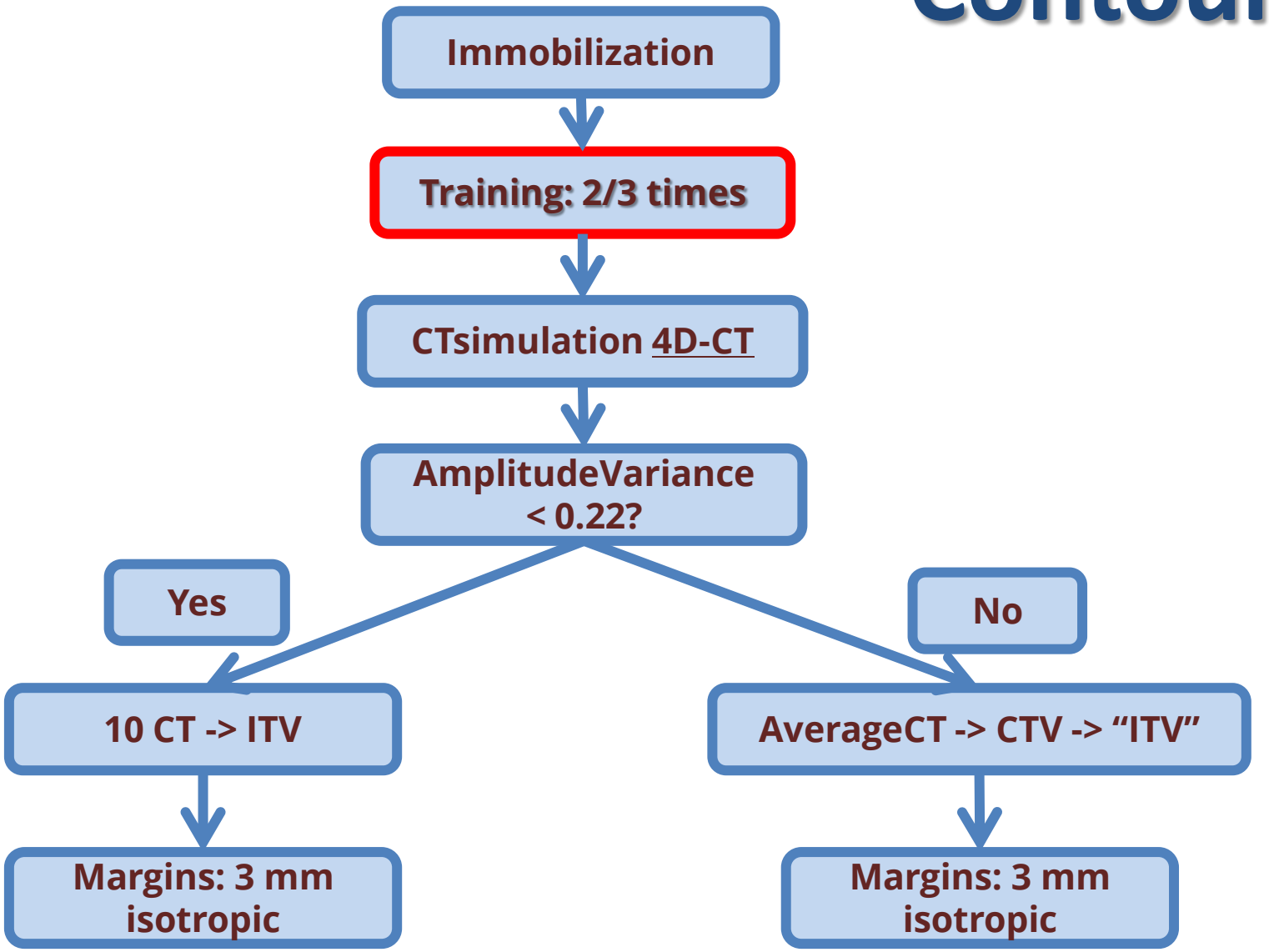
Immobilization
Training: 2/3 times
CTsimulation 4D-CT
AmplitudeVariance < 0.22?
Yes
No
10 CT -> ITV
AverageCT -> CTV -> "ITV"
Margins: 3 mm isotropic
Margins: 3 mm isotropic

Training

ACTIVE BREATHING CONTROL

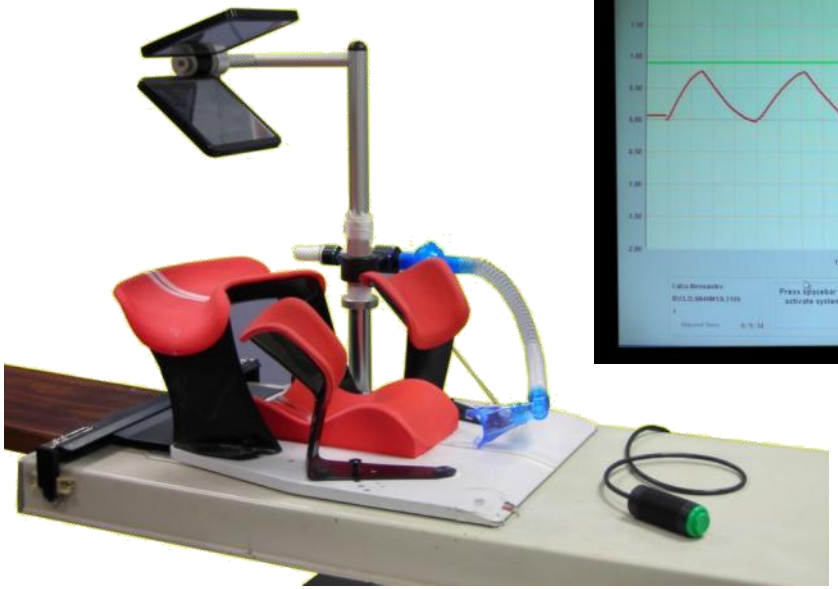

To reduce variability of respiratory movements

during the radiotherapy treatment

Contouring

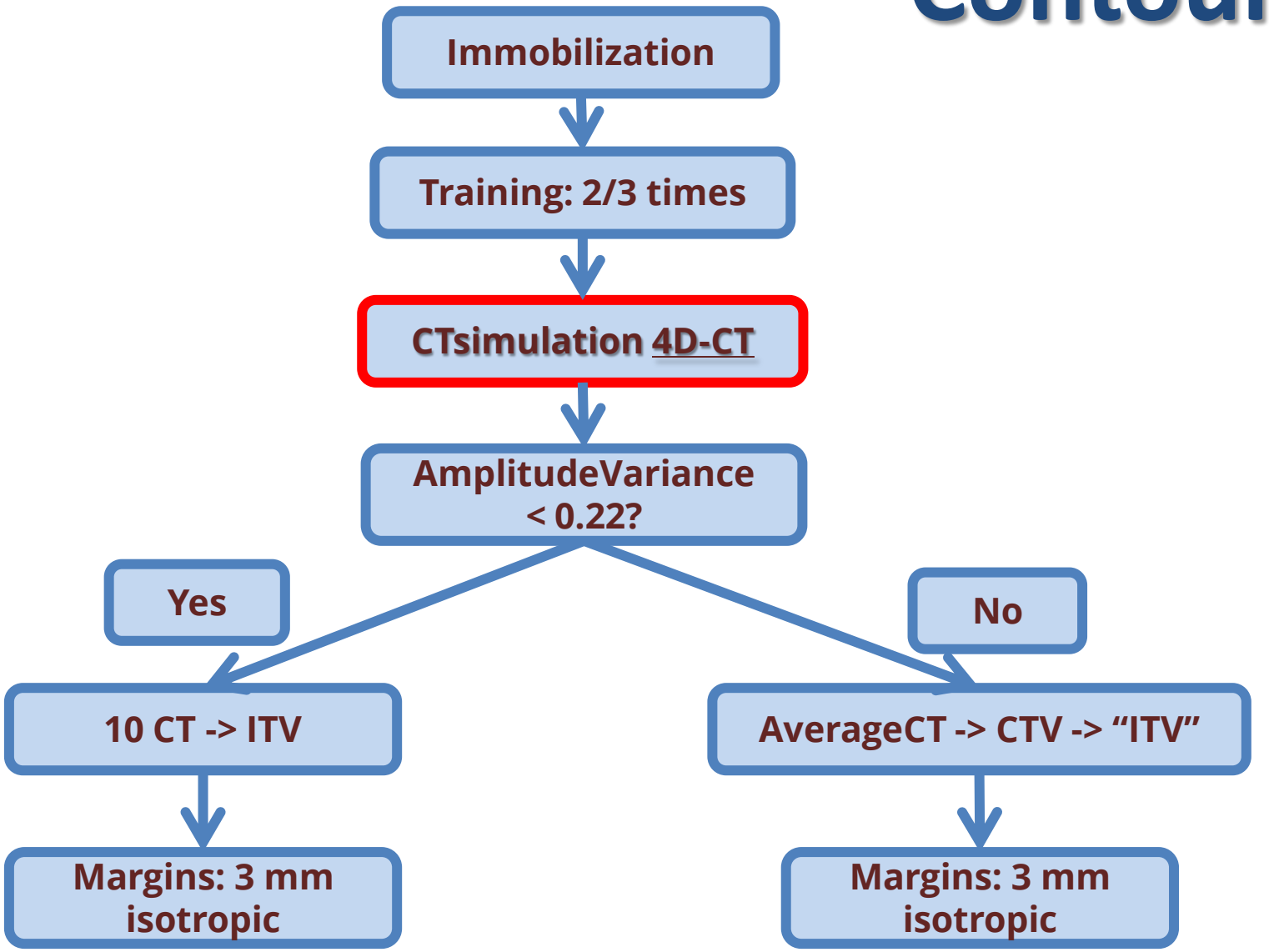
Immobilization
Training: 2/3 times
CTsimulation 4D-CT
AmplitudeVariance < 0.22?
Yes
No
10 CT -> ITV
AverageCT -> CTV -> "ITV"
Margins: 3 mm isotropic
Margins: 3 mm isotropic

CT-Simulation 4D-CT

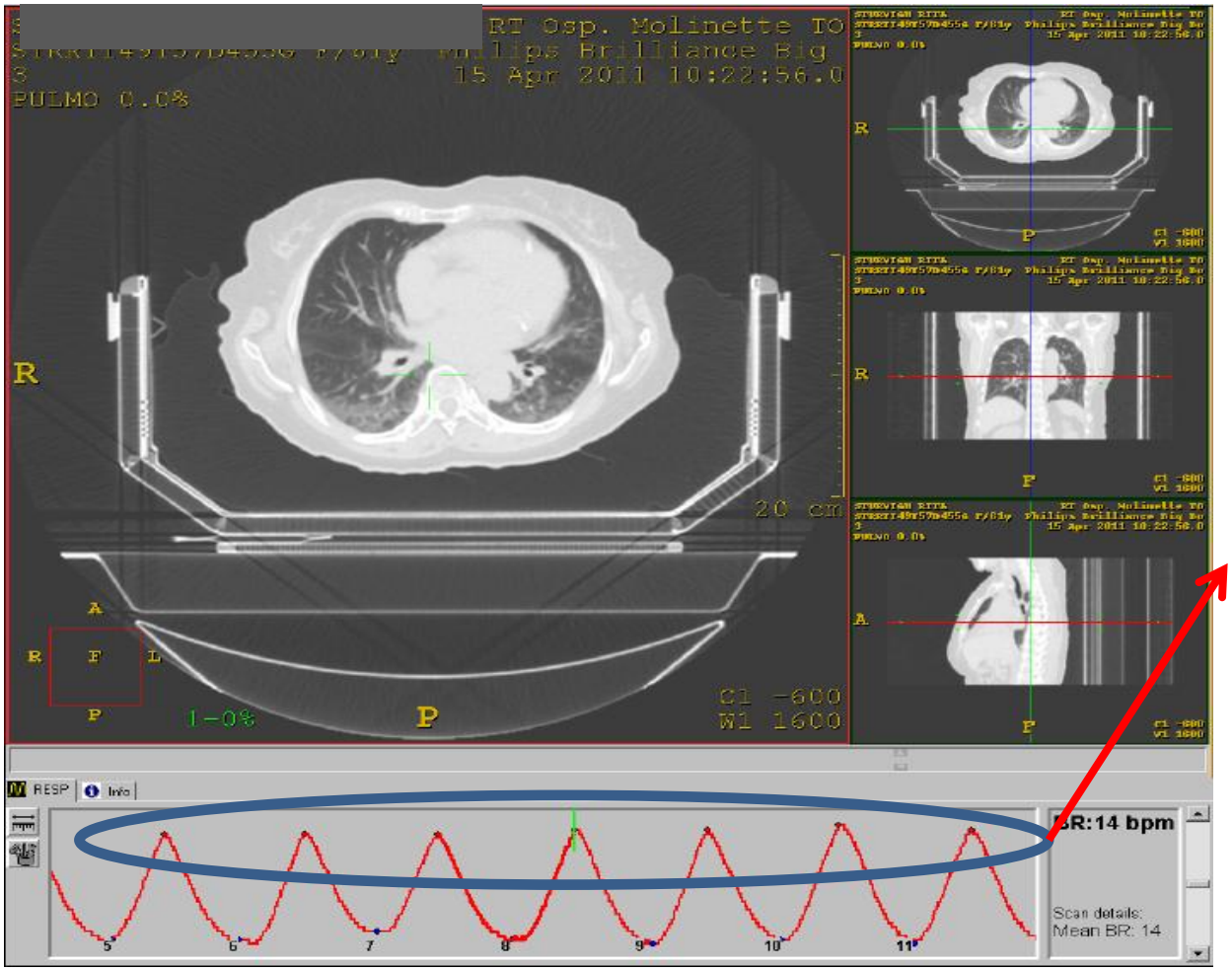

After an analysis of amplitude variance:

We choose as suitable for an accurate 4D-CT the threshold value of **20%** (±10%)

- ***Phase binning***:
10 series of images corresponding to 10 phases of respiratory cycle

Contouring

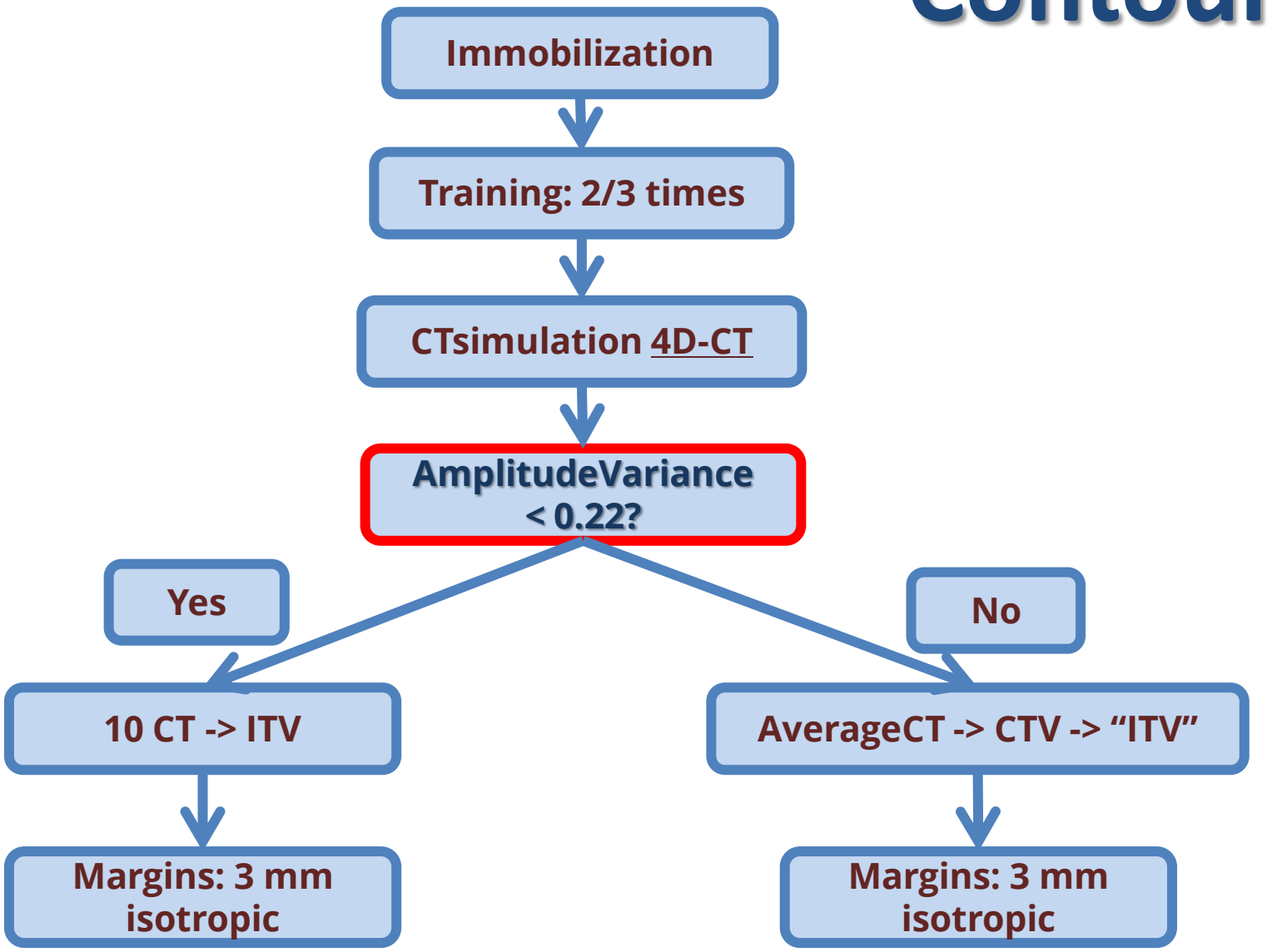
Immobilization
Training: 2/3 times
CTsimulation 4D-CT
AmplitudeVariance < 0.22?
Yes
No
10 CT -> ITV
AverageCT -> CTV -> "ITV"
Margins: 3 mm isotropic
Margins: 3 mm isotropic

AV < 0.22

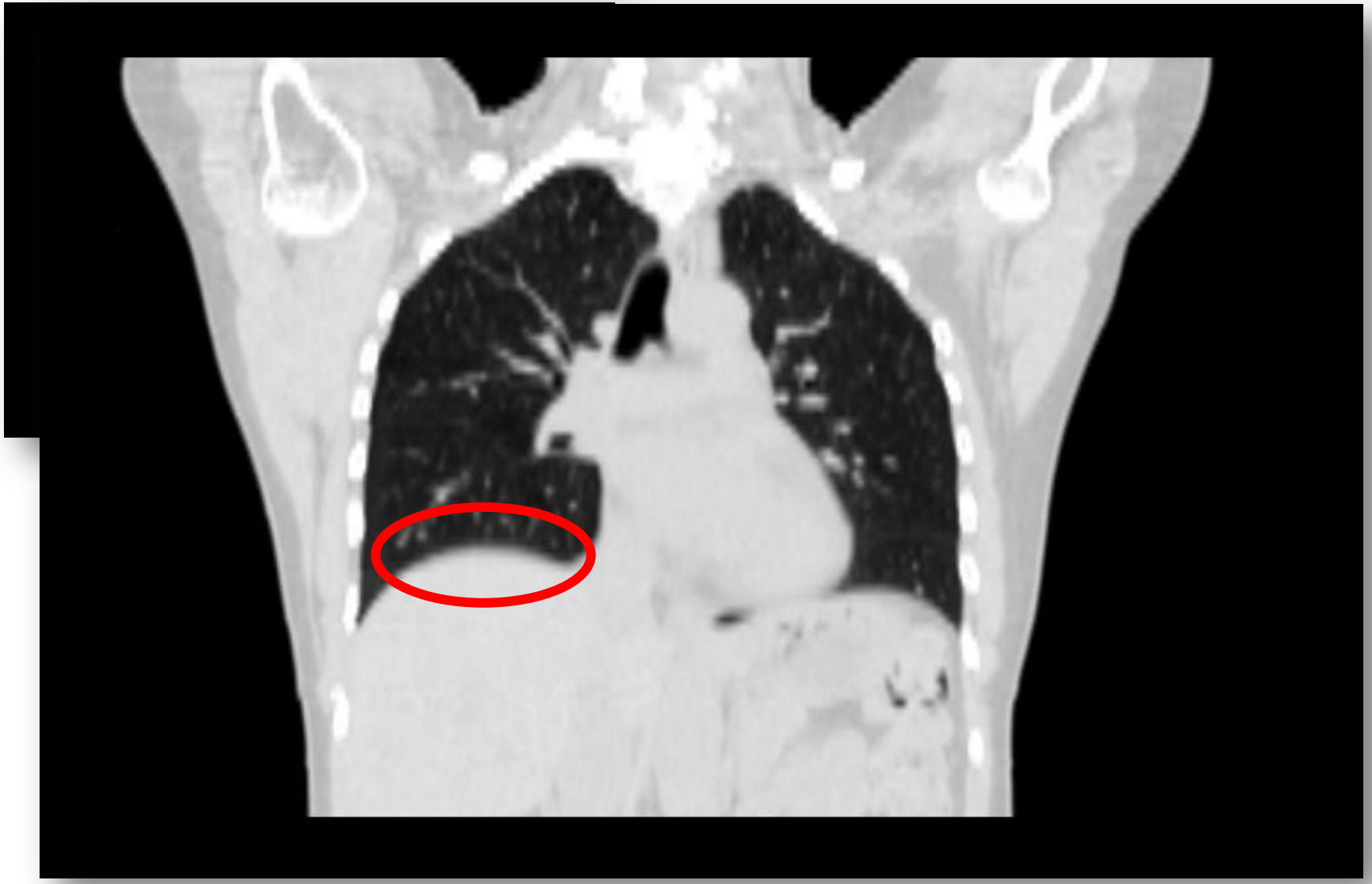

10%

20%

30%

.....

Reference CT (e.g. 0%)

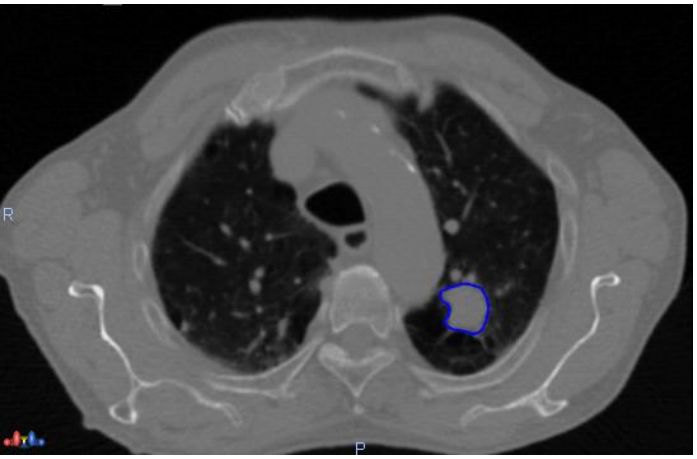

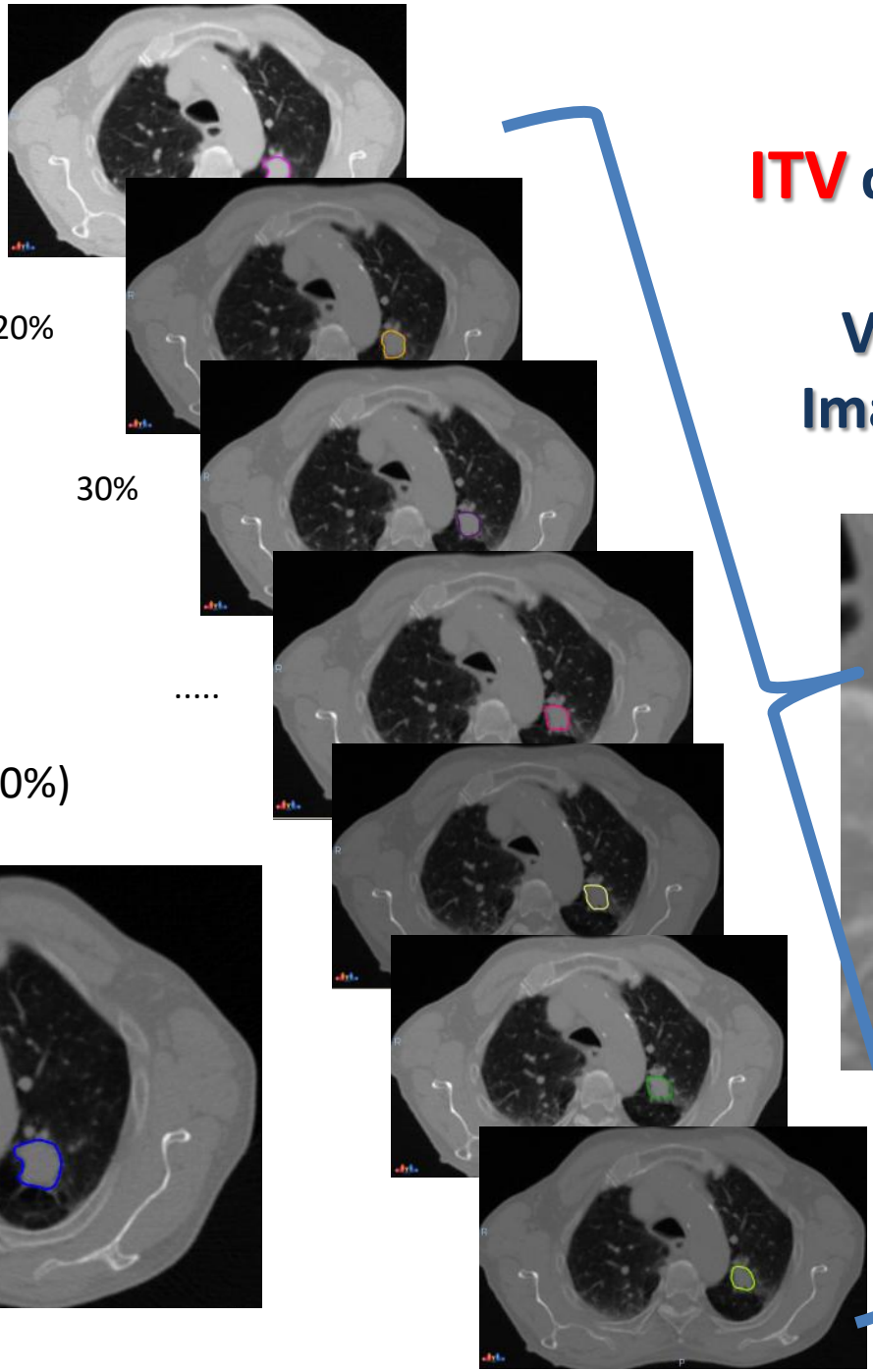

ITV delineation on the Average CT: Via Deformable Image Registration (VelocityAI)

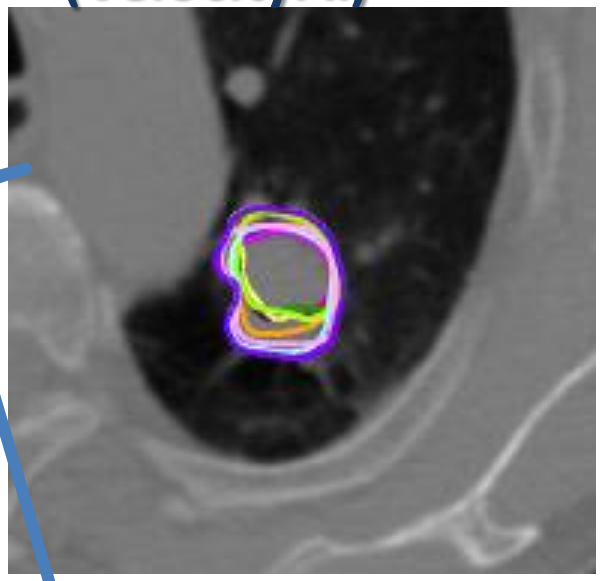

Contouring

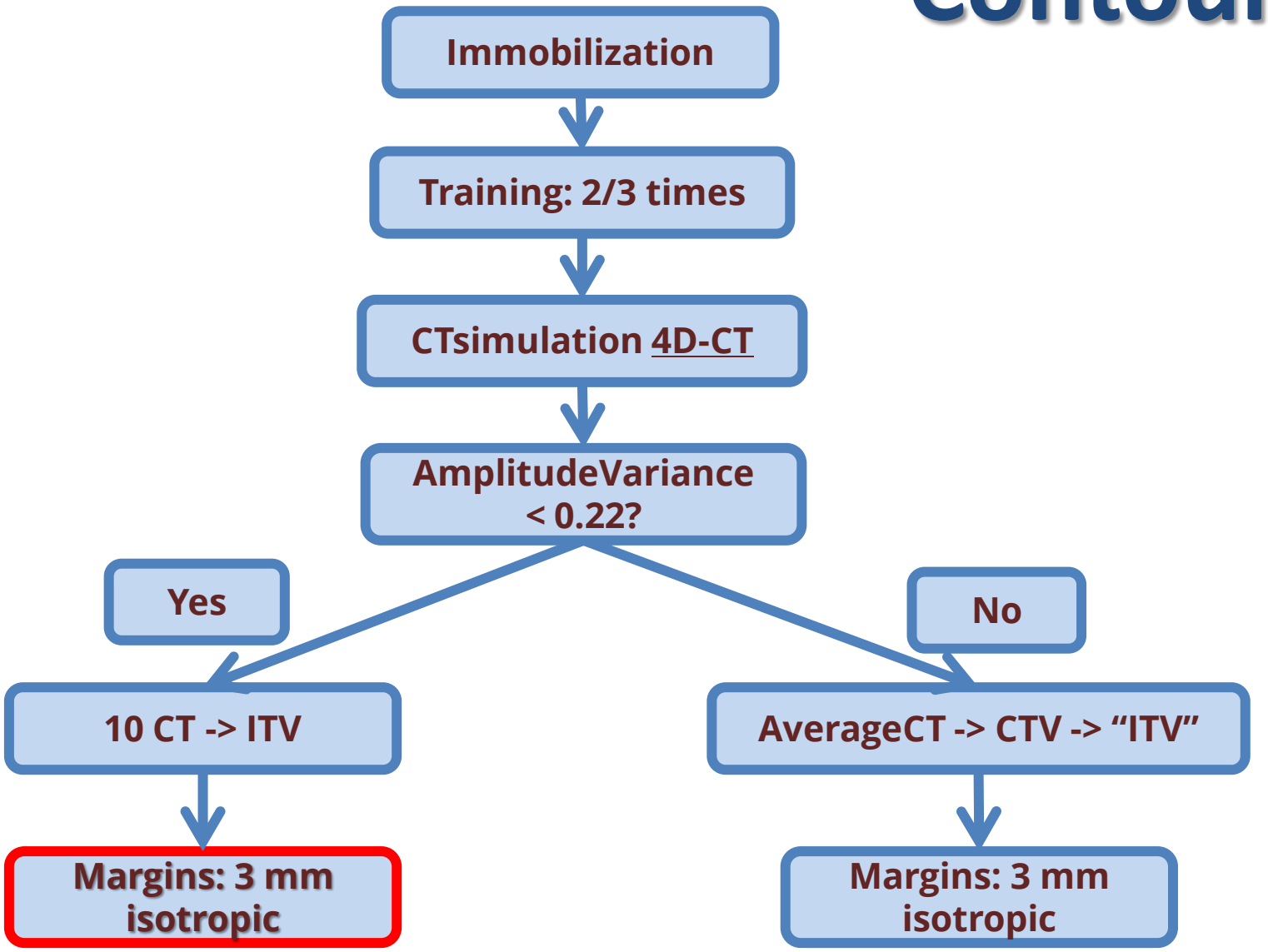
Immobilization
Training: 2/3 times
CTsimulation 4D-CT
AmplitudeVariance < 0.22?
Yes
No
10 CT -> ITV
AverageCT -> CTV -> "ITV"
Margins: 3 mm isotropic
Margins: 3 mm isotropic

Margins

Localization accuracy was quantified by the residual tumor misalignment measured in the second 4D-CBCT scan acquired for validation and expressed in terms of systematic (Σ), and random (σ) errors.

For dose prescription at 80% instead of 95%, for a lung target(σ_p = 0.64):

$$M = 2.5\Sigma + 0.84\sqrt{(\sigma_p^2 + \sigma^2)} - 0.84\sigma_p^2$$

Margins

We calculated:

LL: 1.6 mm

AP: 1.9 mm

CC: 2.4 mm

We choose:

3 mm isotropic (from ITV)

AV > 0.22

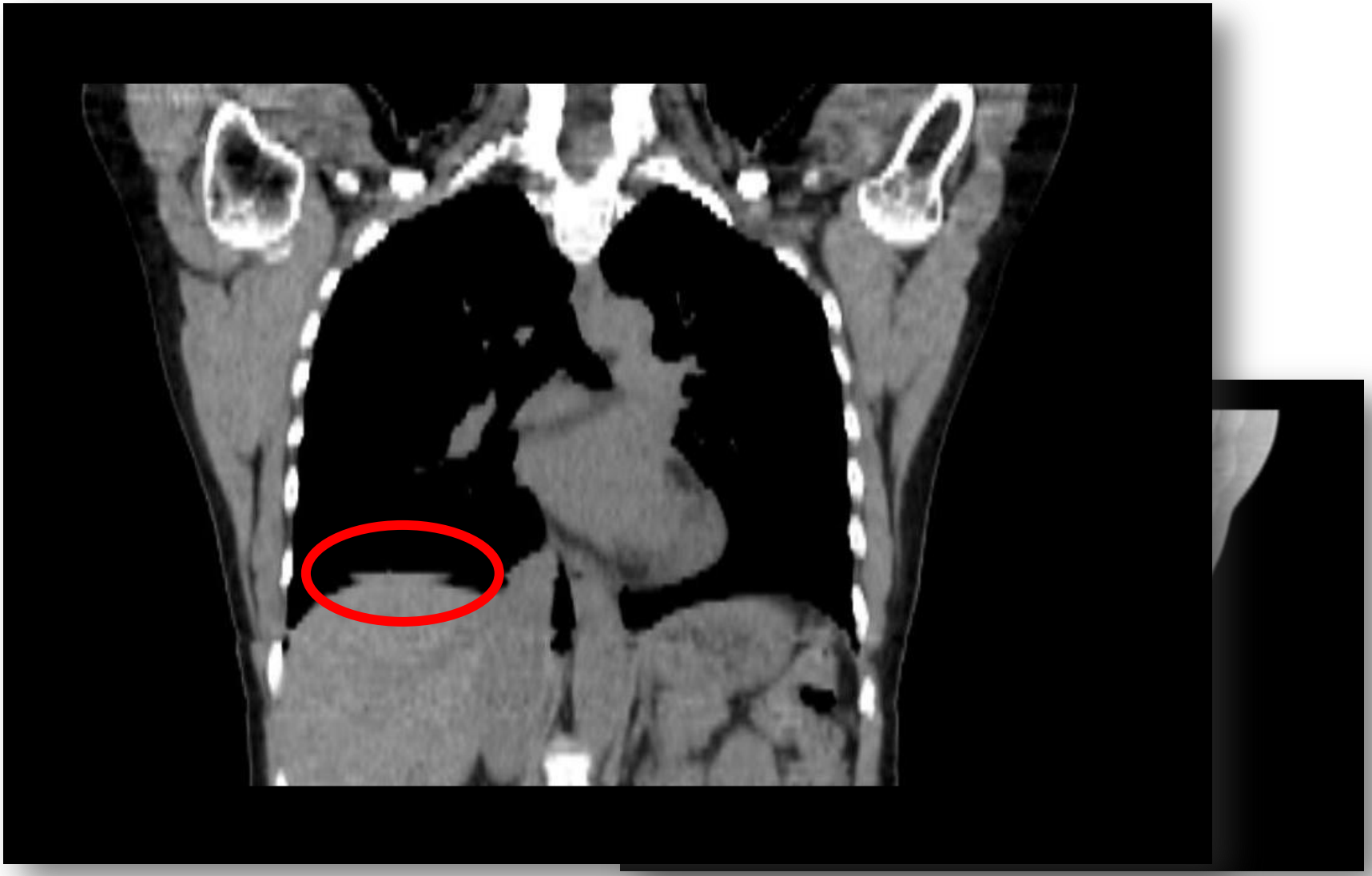

Contouring: 'statistic ITV'

- Contour of CTV on the Average CT obtained from the 4D-CT scan.
- Obtain a 'statistic ITV' (sITV) by adding margins related to the location of the tumor. We based the amplitude of these margins on a statistical analysis of the tumor motion. Then we used the mean value and 2 SD to define margins for each lobe and for each axis:

➢ Inferior lobe(cm):	LL: **0.11**	AP: **0.43**	CC: **0.65**
➢ Medium lobe(cm):	LL: **0.10**	AP: **0.35**	CC: **0.60**
➢ Superior lobe(cm):	LL: **0.10**	AP: 0.**34**	CC: **0.58**

- Then we add **3 mm isotropic** (from sITV) to obtain PTV

Planning and Delivery

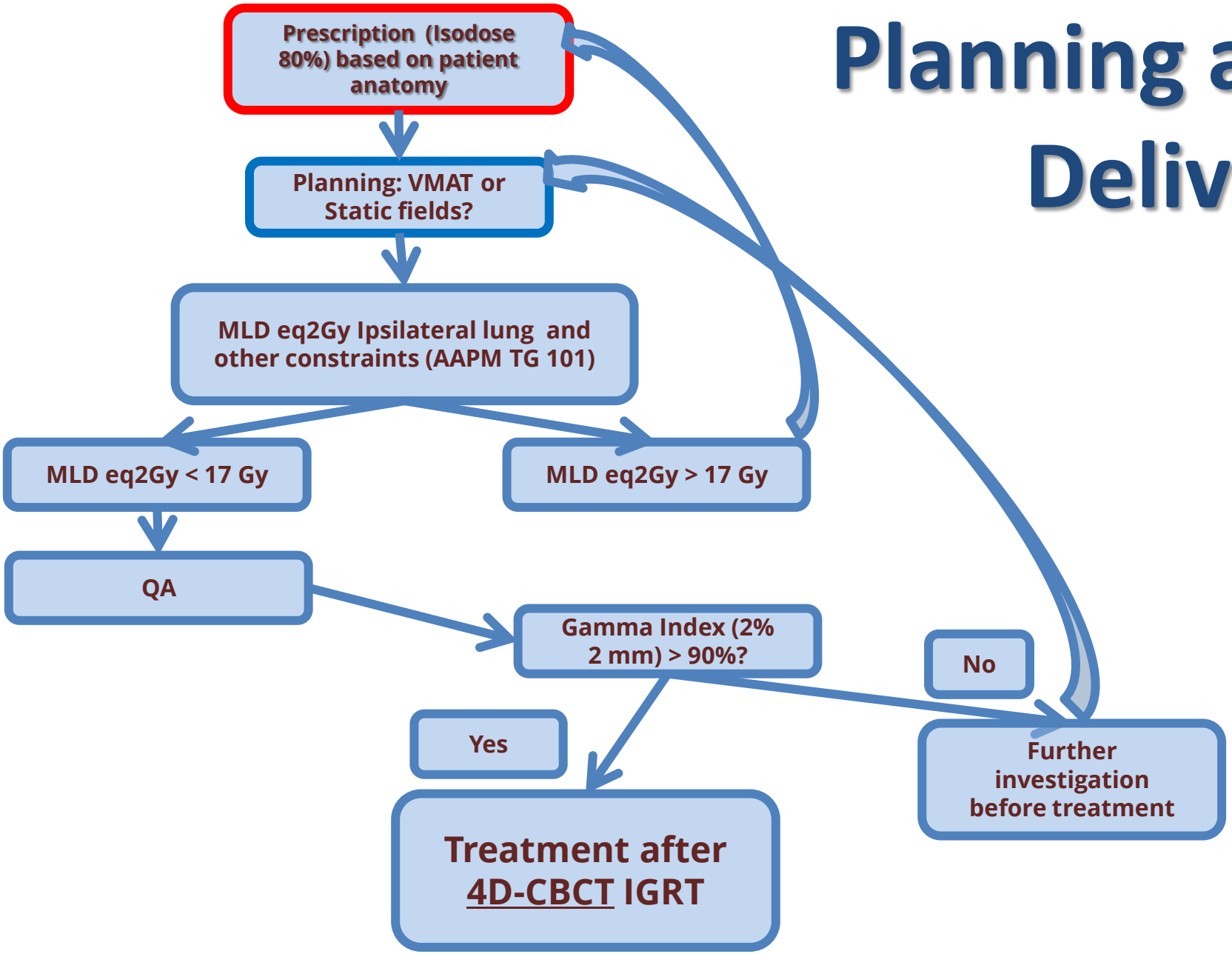

Prescriptions

Clinical routine: “risk-adapted” SBRT protocol

- **Peripheral lesions (T1a-T1b):**

- 45-54 Gy/ 3 fractions

- **Peripheral lesions, with extensive contact with the chest wall, or larger tumors (T2a):**

- 55 Gy/ 5 fractions

- **Central lesions:**

- 60 Gy/ 8 fractions

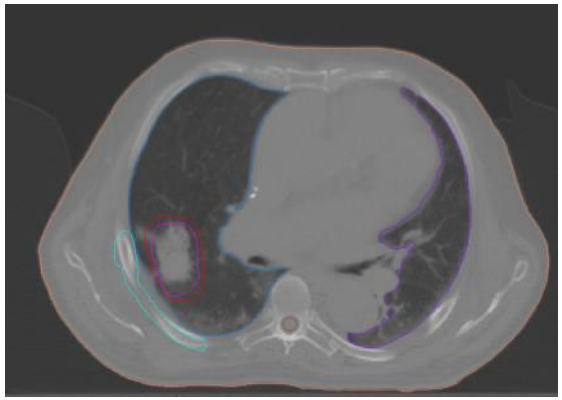

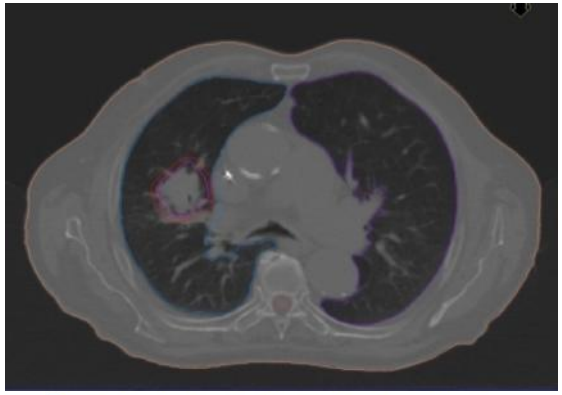

DEPARTMENT OF
ONCOLOGY
UNIVERSITY OF TURIN

Planning and Delivery

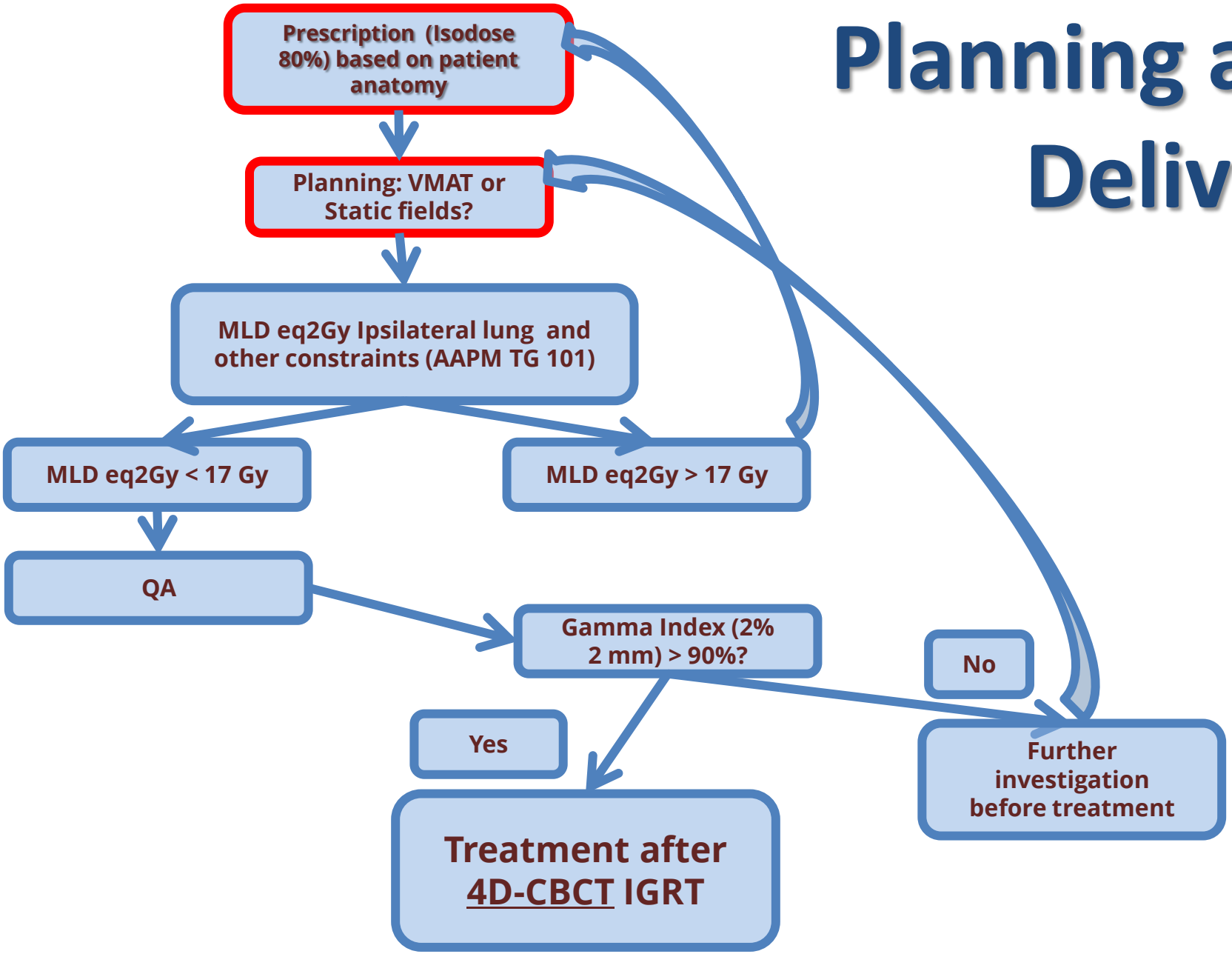

Step & Shoot or VMAT?

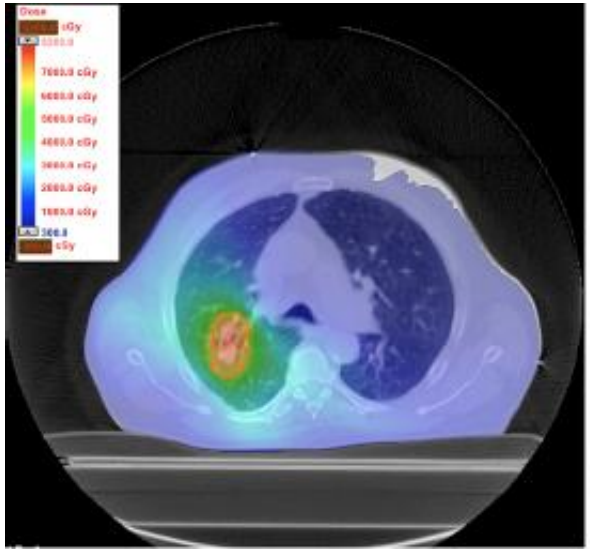

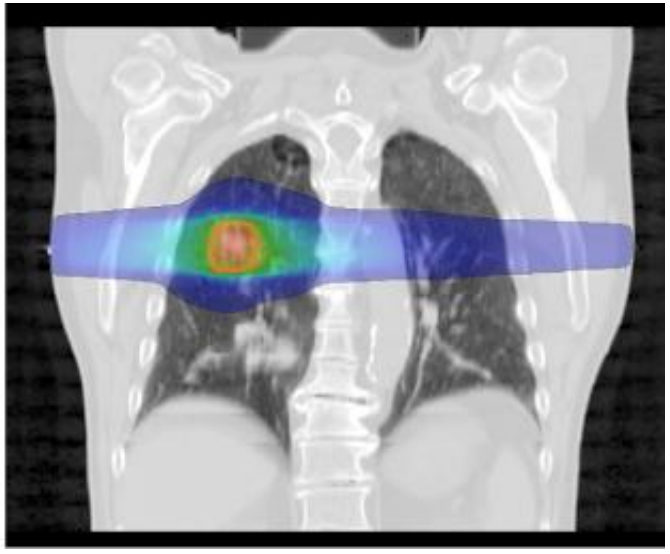

Planning with:
Elekta CMS
Monaco v.3.2/3.3

Grid calculation 2 mm,
Montecarlo Variance 1.5%

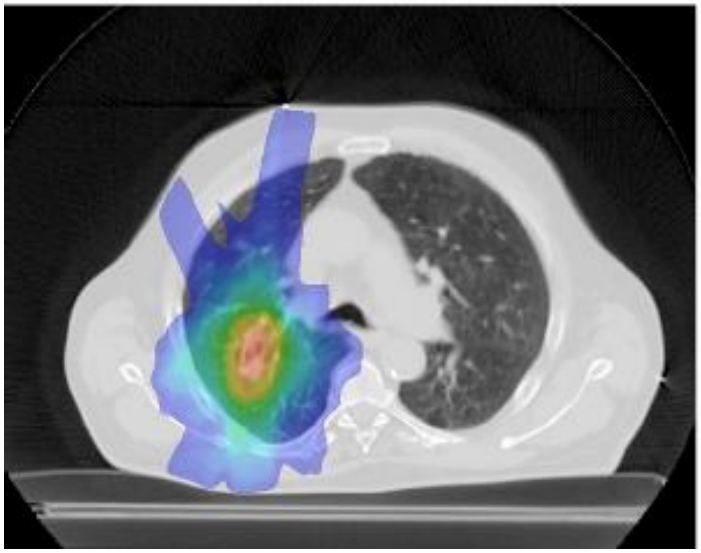

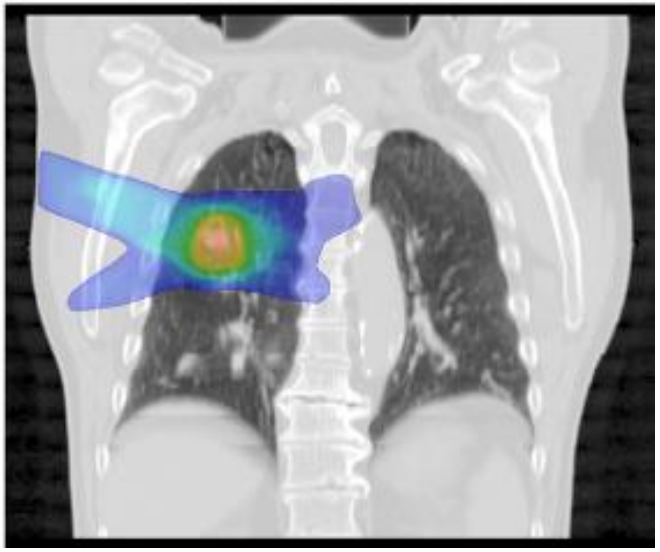

Planning and Delivery

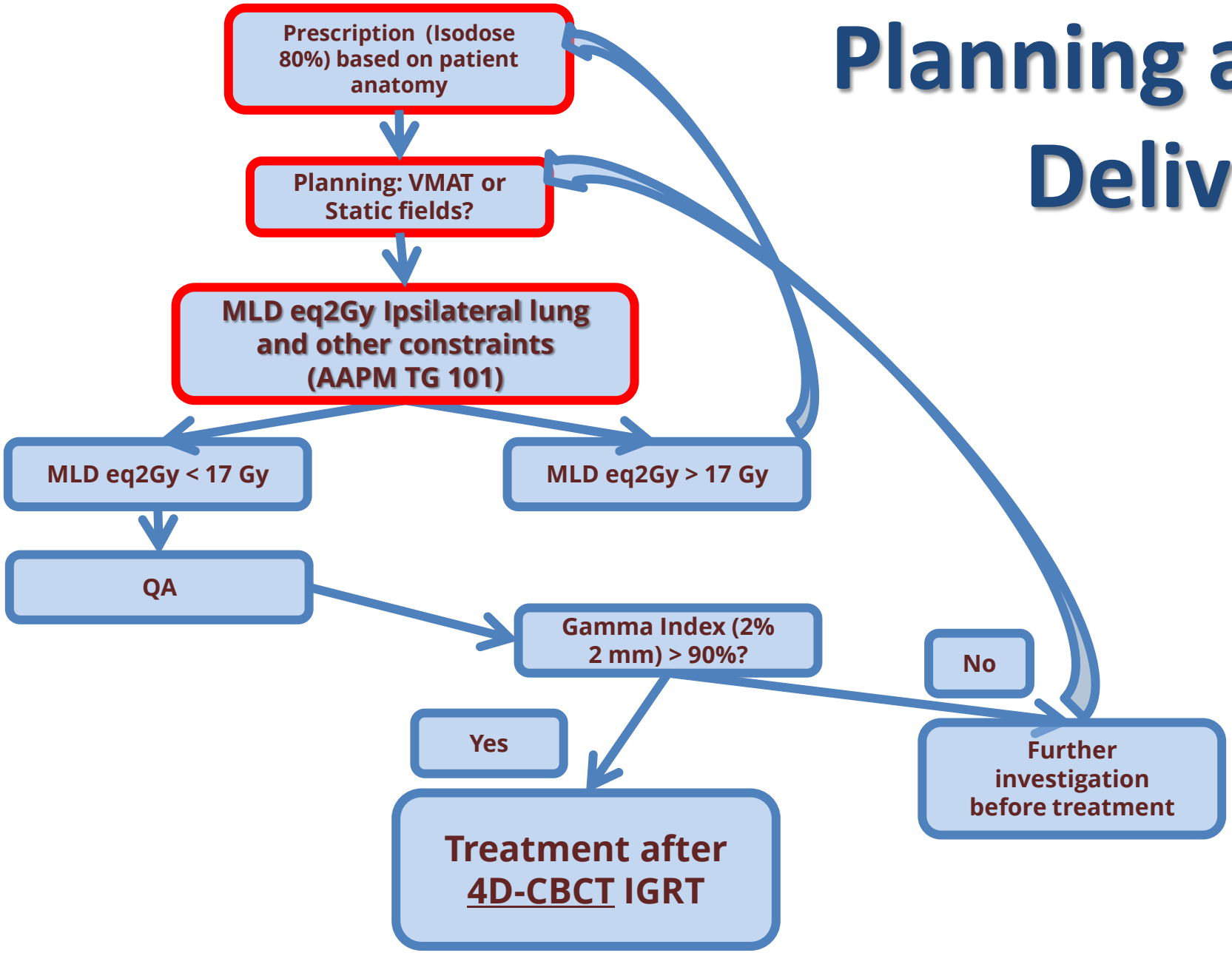

MLD_{2Gy} Ipsilateral Lung

Table IV. Logistic regression analysis (correlation with RTOG grade 2-3 pulmonary toxicity)

	Odds Ratio	Std. Err.	z	p	95% Confidence Interval	
MLD_2	**1.52**	0.24	2.66	**0.008**	1.12	2.08
Primary/ Metastatic	3.03	3.98	0.84	0.399	0.23	39.79
Central/Peripheral	0.54	0.70	−0.48	0.634	0.04	6.75
Superior/Median/Inferior Lobe	1.53	0.89	0.73	0.464	0.49	4.79
PTV	1.03	0.03	1.05	0.293	0.98	1.08

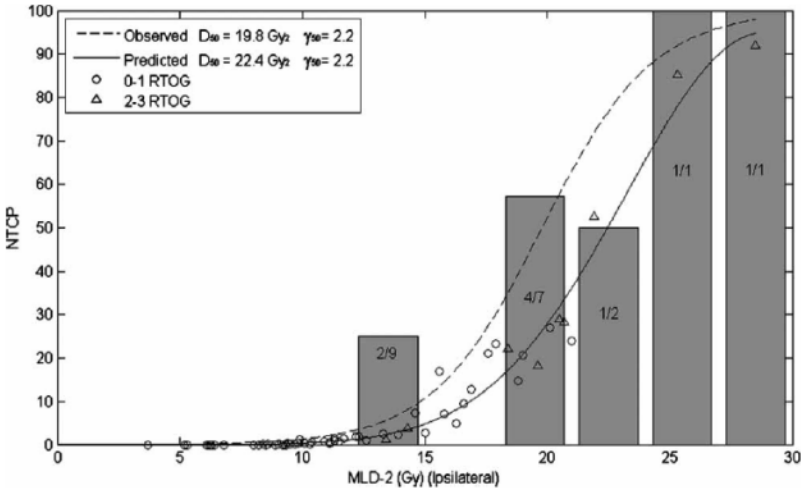

Table III. MLD_2 and NTCP mean values according to RTOG lung toxicity score

	Grade 0-1	Grade 2-3
MLD_2	**11.2 Gy** (95% CI 10.1-12.3 Gy)	**20.3 Gy** (95% CI 16.6-23.9 Gy)
NTCP	**4%** (95% CI 2-5.9%)	**37%** (95% CI 11.6-62.3%)

Dosimetric predictors of radiation-induced lung injury in stereotactic body radiation therapy

Acta Oncologica, 2009; 48: 571–577

MLD_{2Gy} Ipsilateral Lung

Decomposition analysis of differential dose volume histograms

Frank Van den Heuvel Ph.D.[a)]
Department of Oncology and Experimental Radiation Therapy
Universiteit Leuven, Belgium

Dose volume histograms are a common tool to assess the value of a treatment plan for various forms of radiation therapy treatment. The purpose of this work is to introduce, validate, and apply a set of tools to analyze differential dose volume histograms by decomposing them into physically and clinically meaningful normal distributions. A weighted sum of the decomposed normal distributions (e.g. weighted dose) is proposed as a new measure of target dose, rather than the more unstable point dose.

The method and its theory are presented and validated using simulated distributions. Additional validation is performed by analyzing simple four field box techniques encompassing a pre–defined target, using different treatment energies inside a waterphantom.

Furthermore, two clinical situations are analyzed using this methodology to illustrate practical usefulness. A comparison of a treatment plan for a breast patient using a tangential field setup with wedges is compared to a comparable geometry using dose compensators. Finally, a normal tissue complication probability (NTCP) calculation is refined using this decomposition. The NTCP calculation is performed on a liver as organ at risk in a treatment of a mesothelioma patient with involvement of the right lung.

The comparison of the wedged breast treatment versus the compensator technique yields comparable classical dose parameters (e.g Conformity Index ≈ 1 and equal dose at the ICRU dose point). The methodology proposed here shows a 4% difference in weighted dose outlining the difference in treatment using a single parameter instead of at least two in a classical analysis (e.g. mean dose, and maximal dose, or total dose variance). NTCP–calculations for the mesothelioma case are generated automatically and show a 3% decrease with respect to the classical calculation. The decrease is slightly dependant on the fractionation and on the α/β–value utilized.

In conclusion, this method is able to distinguish clinically important differences between treatment plans using a single parameter. This methodology shows promise as an objective tool for analyzing NTCP and doses in larger studies, as the only information needed is the dose volume histogram.

Constraints

Stereotactic body radiation therapy: The report of AAPM Task Group 101

Stanley H. Benedict, Chairman[a)]
University of Virginia Health System, Charlottesville, Virginia 22908

TABLE III. Summary of suggested dose constraints for various critical organs. Note that for serial tissues, the volume-dose constraints are given in terms of the critical maximum tissue volume that should receive a dose equal or greater than the indicated threshold dose for the given number of fractions used. For parallel tissue, the volume-dose constraints are based on a critical minimum volume of tissue that should receive a dose equal to or less than the indicated threshold dose for the given number of fractions used.

		One fraction		Three fractions		Five fractions		
Serial tissue	Max critical volume above threshold	Threshold dose (Gy)	Max point dose (Gy)[a]	Threshold dose (Gy)	Max point dose (Gy)[a]	Threshold dose (Gy)	Max point dose (Gy)[a]	End point (≥Grade 3)
Optic pathway	<0.2 cc	8	10	15.3 (5.1 Gy/fx)	17.4 (5.8 Gy/fx)	23 (4.6 Gy/fx)	25 (5 Gy/fx)	Neuritis
Cochlea			9		17.1 (5.7 Gy/fx)		25 (5 Gy/fx)	Hearing loss
Brainstem (not medulla)	<0.5 cc	10	15	18 (6 Gy/fx)	23.1 (7.7 Gy/fx)	23 (4.6 Gy/fx)	31 (6.2 Gy/fx)	Cranial neuropathy
Spinal cord and medulla	<0.35 cc <1.2 cc	10 7	14	18 (6 Gy/fx) 12.3 (4.1 Gy/fx)	21.9 (7.3 Gy/fx)	23 (4.6 Gy/fx) 14.5 (2.9 Gy/fx)	30 (6 Gy/fx)	Myelitis
Spinal cord sub volume (5–6 mm above and below level treated per Ryu)	<10% of subvolume	10	14	18 (6 Gy/fx)	21.9 (7.3 Gy/fx)	23 (4.6 Gy/fx)	30 (6 Gy/fx)	Myelitis
Cauda equina	<5 cc	14	16	21.9 (7.3 Gy/fx)	24 (8 Gy/fx)	30 (6 Gy/fx)	32 (6.4 Gy/fx)	Neuritis
Sacral plexus	<5 cc	14.4	16	22.5 (7.5 Gy/fx)	24 (8 Gy/fx)	30 (6 Gy/fx)	32 (6.4 Gy/fx)	Neuropathy
Esophagus[b]	<5 cc	11.9	15.4	17.7 (5.9 Gy/fx)	25.2 (8.4 Gy/fx)	19.5 (3.9 Gy/fx)	35 (7 Gy/fx)	Stenosis/fistula
Brachial plexus	<3 cc	14	17.5	20.4 (6.8 Gy/fx)	24 (8 Gy/fx)	27 (5.4 Gy/fx)	30.5 (6.1 Gy/fx)	Neuropathy
Heart/pericardium	<15 cc	16	22	24 (8 Gy/fx)	30 (10 Gy/fx)	32 (6.4 Gy/fx)	38 (7.6 Gy/fx)	Pericarditis
Great vessels	<10 cc	31	37	39 (13 Gy/fx)	45 (15 Gy/fx)	47 (9.4 Gy/fx)	53 (10.6 Gy/fx)	Aneurysm
Trachea and large bronchus[b]	<4 cc	10.5	20.2	15 (5 Gy/fx)	30 (10 Gy/fx)	16.5 (3.3 Gy/fx)	40 (8 Gy/fx)	Stenosis/fistula
Bronchus-smaller airways	<0.5 cc	12.4	13.3	18.9 (6.3 Gy/fx)	23.1 (7.7 Gy/fx)	21 (4.2 Gy/fx)	33 (6.6 Gy/fx)	Stenosis with atelectasis
Rib	<1 cc <30 cc	22	30	28.8 (9.6 Gy/fx) 30.0 (10.00 Gy/fx)	36.9 (12.3 Gy/fx)	35 (7 Gy/fx)	43 (8.6 Gy/fx)	Pain or fracture
Skin	<10 cc	23	26	30 (10 Gy/fx)	33 (11 Gy/fx)	36.5 (7.3 Gy/fx)	39.5 (7.9 Gy/fx)	Ulceration
Stomach	<10 cc	11.2	12.4	16.5 (5.5 Gy/fx)	22.2 (7.4 Gy/fx)	18 (3.6 Gy/fx)	32 (6.4 Gy/fx)	Ulceration/fistula
Duodenum[b]	<5 cc <10 cc	11.2 9	12.4	16.5 (5.5 Gy/fx) 11.4 (3.8 Gy/fx)	22.2 (7.4 Gy/fx)	18 (3.6 Gy/fx) 12.5 (2.5 Gy/fx)	32 (6.4 Gy/fx)	Ulceration
Jejunum/ileum[b]	<5 cc	11.9	15.4	17.7 (5.9 Gy/fx)	25.2 (8.4 Gy/fx)	19.5 (3.9 Gy/fx)	35 (7 Gy/fx)	Enteritis/ obstruction
Colon[b]	<20 cc	14.3	18.4	24 (8 Gy/fx)	28.2 (9.4 Gy/fx)	25 (5 Gy/fx)	38 (7.6 Gy/fx)	Colitis/fistula
Rectum[b]	<20 cc	14.3	18.4	24 (8 Gy/fx)	28.2 (9.4 Gy/fx)	25 (5 Gy/fx)	38 (7.6 Gy/fx)	Proctitis/fistula
Bladder wall	<15 cc	11.4	18.4	16.8 (5.6 Gy/fx)	28.2 (9.4 Gy/fx)	18.3 (3.65 Gy/fx)	38 (7.6 Gy/fx)	Cystitis/fistula
Penile bulb	<3 cc	14	34	21.9 (7.3 Gy/fx)	42 (14 Gy/fx)	30 (6 Gy/fx)	50 (10 Gy/fx)	Impotence
Femoral heads (right and left)	<10 cc	14		21.9 (7.3 Gy/fx)		30 (6 Gy/fx)		Necrosis
Renal hilum/vascular trunk	<2/3 volume	10.6	18.6 (6.2 Gy/fx)			23 (4.6 Gy/fx)		Malignant hypertension

Planning and Delivery

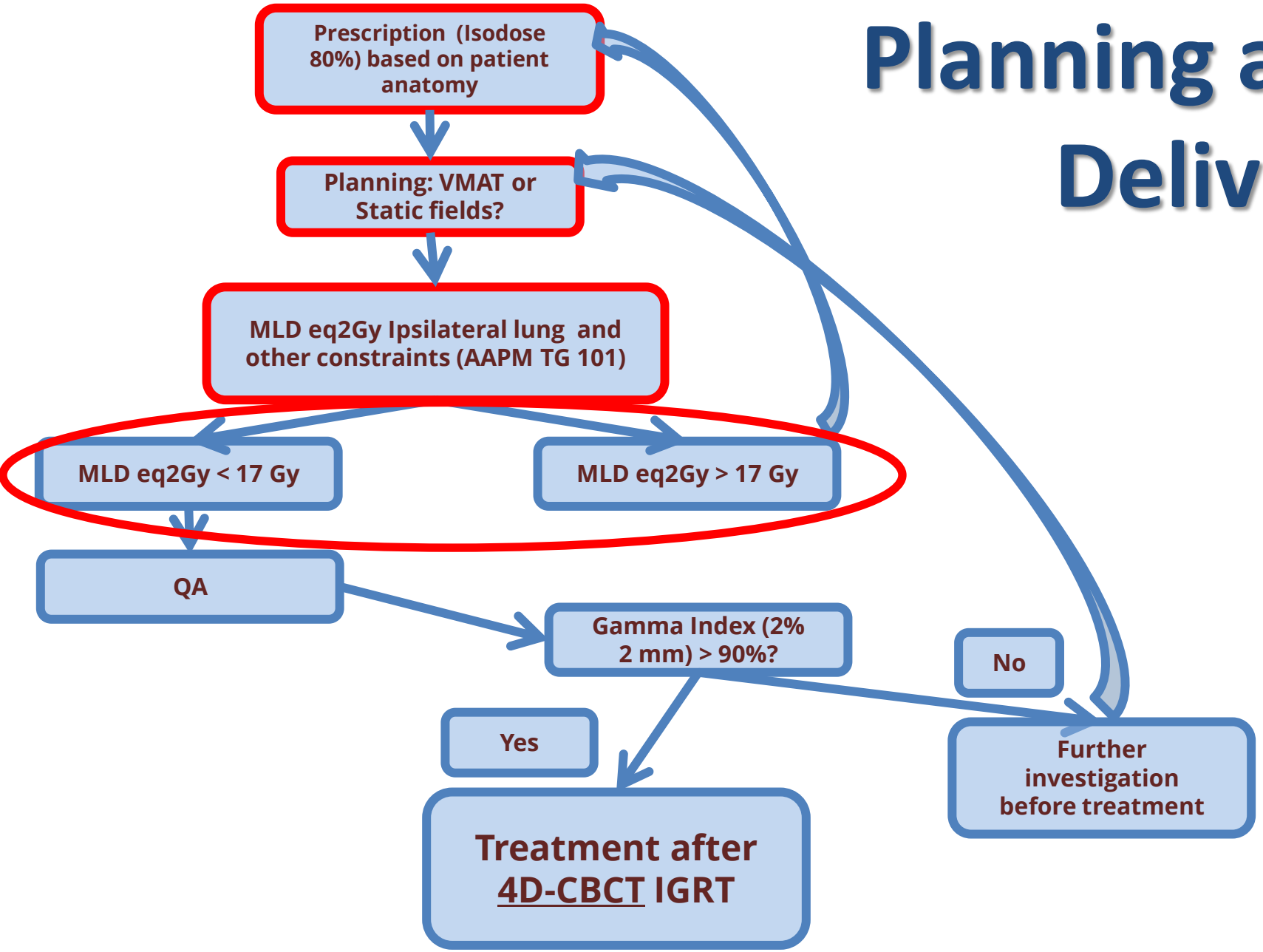

Planning and Delivery

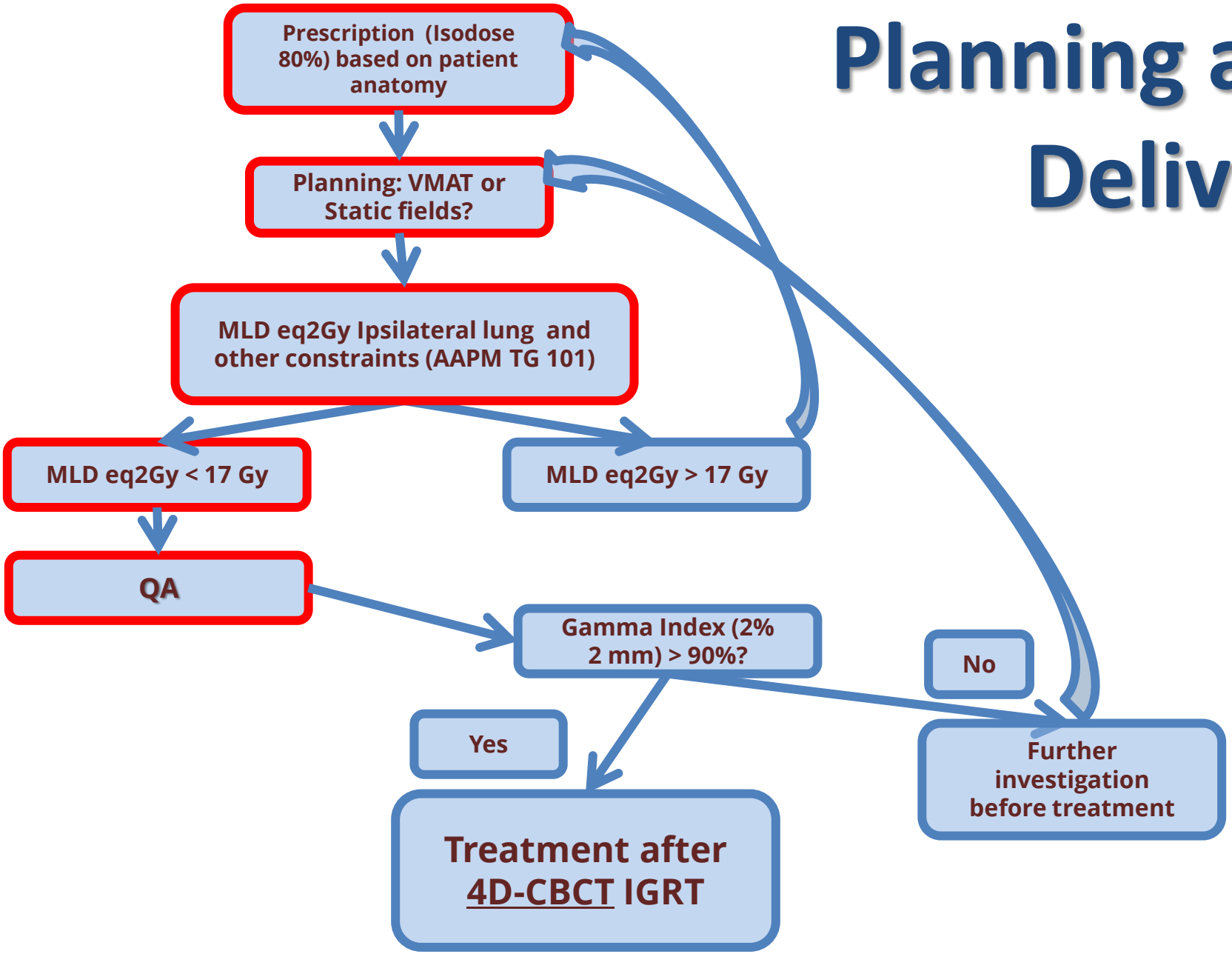

Patient Specific pre-treatment QA: Delta 4

Acceptance level:

- 1 step: 2mm/2% > 90%
- 2 step 3mm/3% > 95%

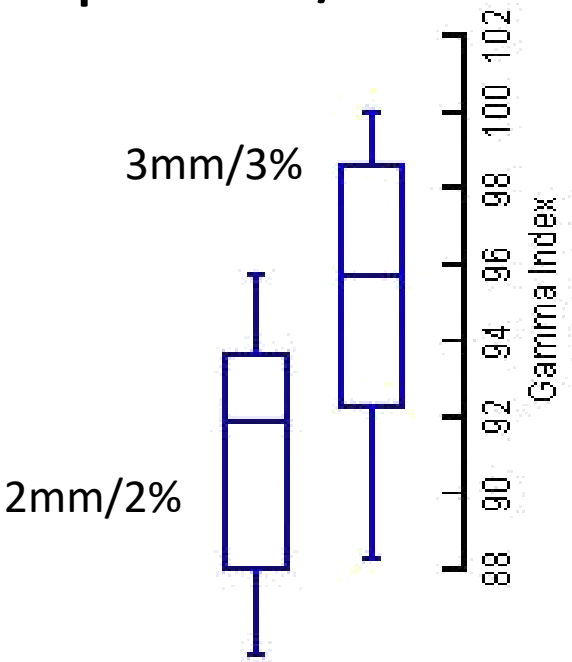

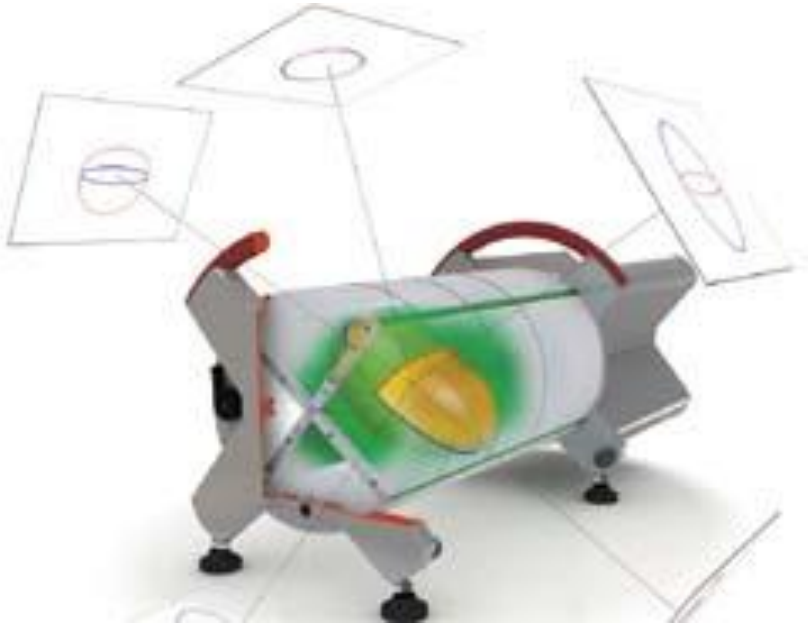

Planning and Delivery

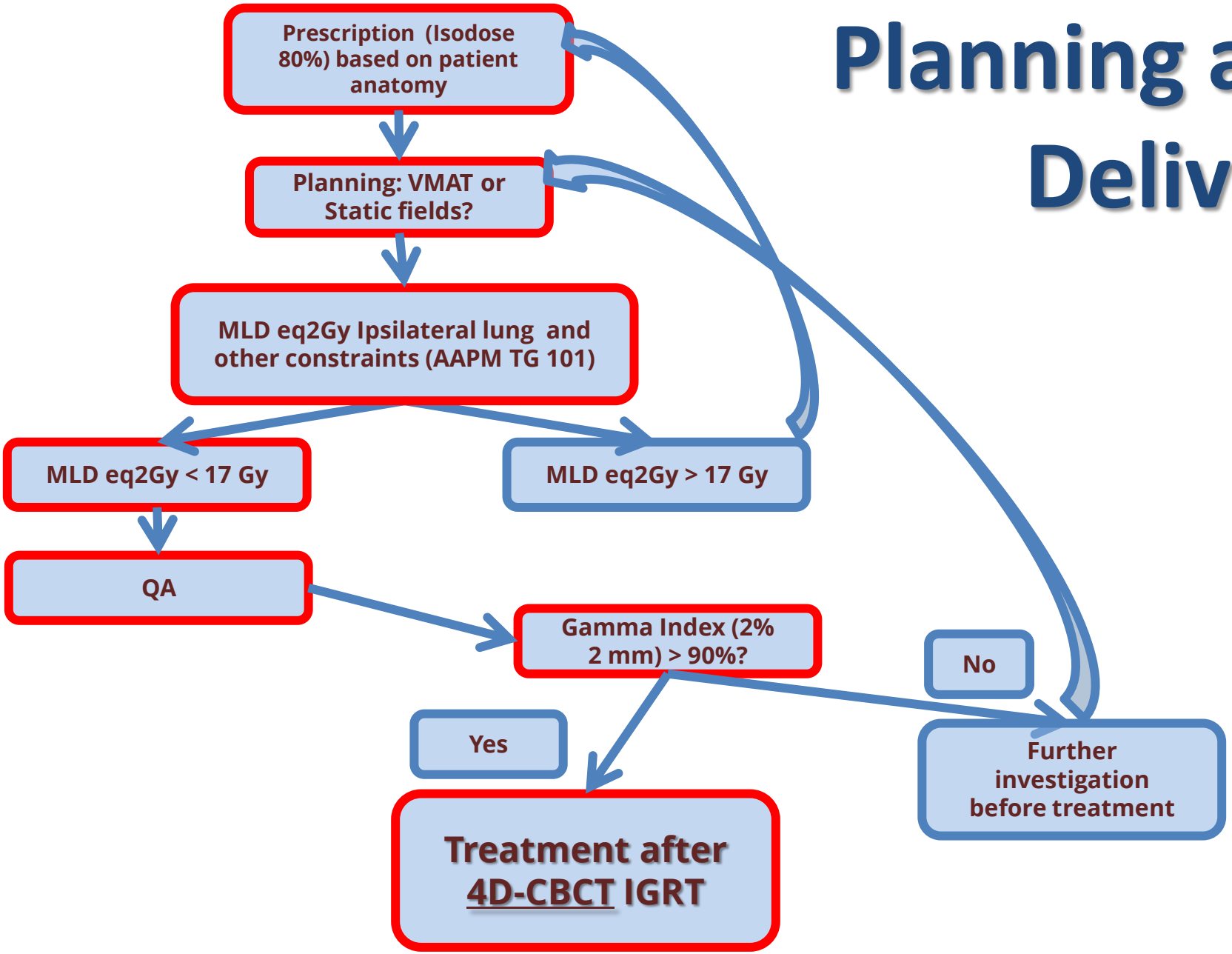

4D –CBCT (XVI v 4.5) at Axesse®,Elekta

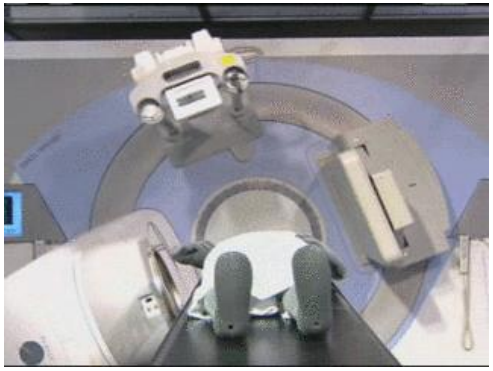

Robotic Couch 6-D: Hexapod

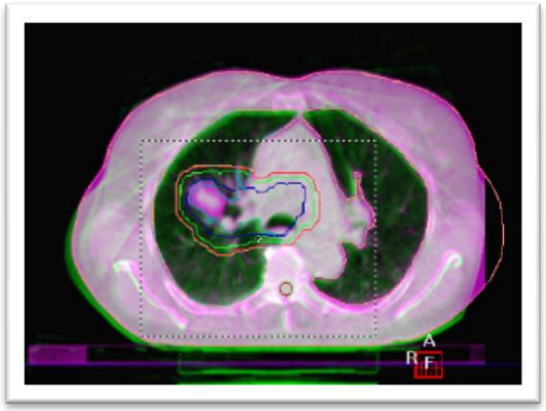

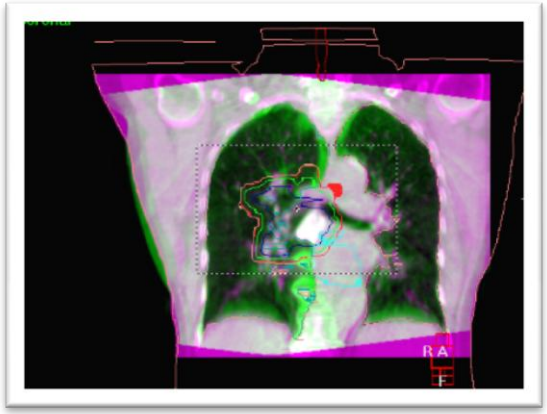

4D-CBCT: correction protocol

First, the bony anatomy was rigidly registered using a user-defined 3D rectangular-shaped **ROI**.

We correct <u>set-up</u> of the patient.

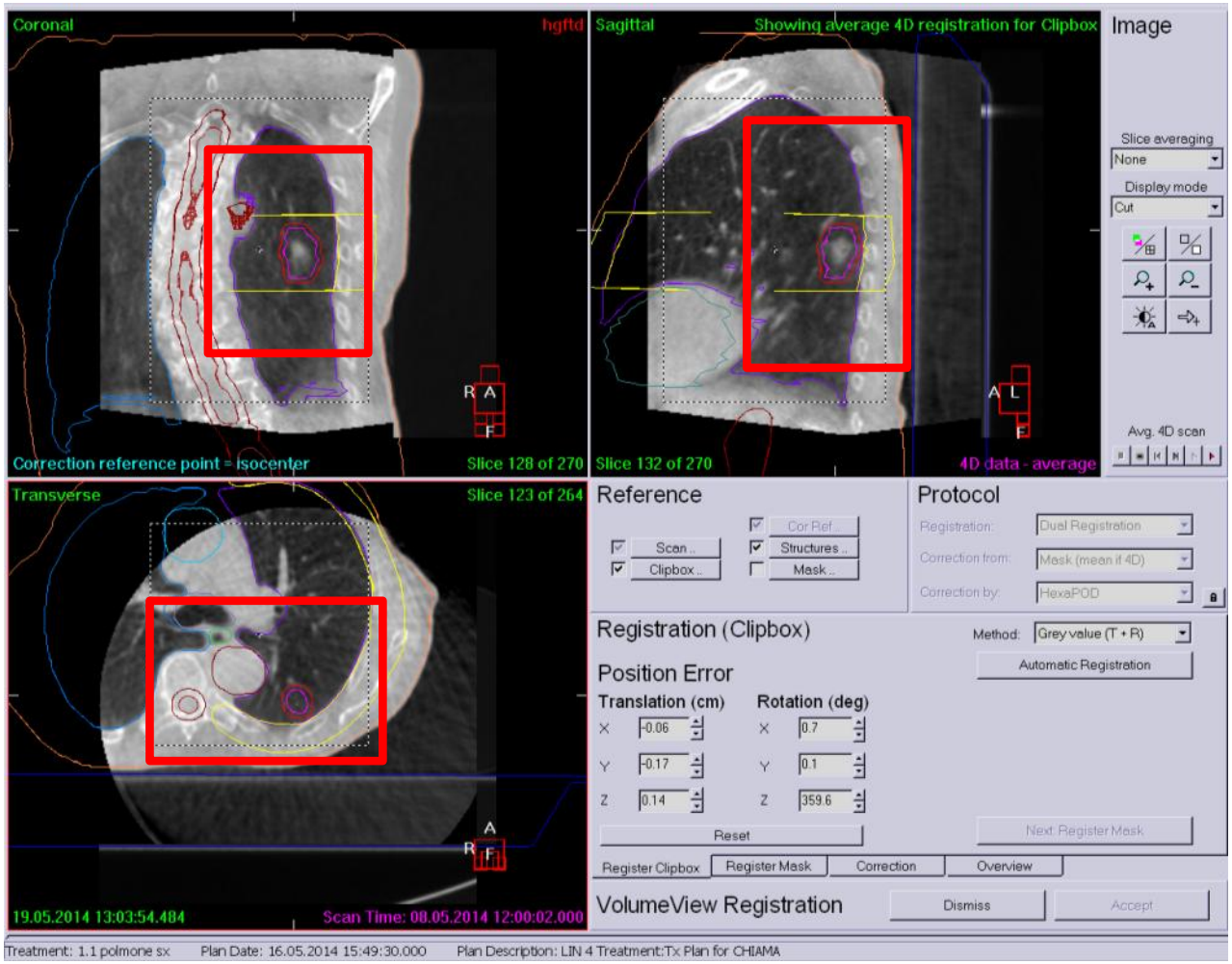

4D-CBCT: correction protocol

- Second, tumor motion analysis was performed using a local rigid registration , based on a 3D-shaped ROI (**PTV expanded by 1.5 cm**)

- This ROI was automatically registered (translations only) to each phase of a 4D-CBCT scan yielding the tumor trajectory relative to the planned tumor position.

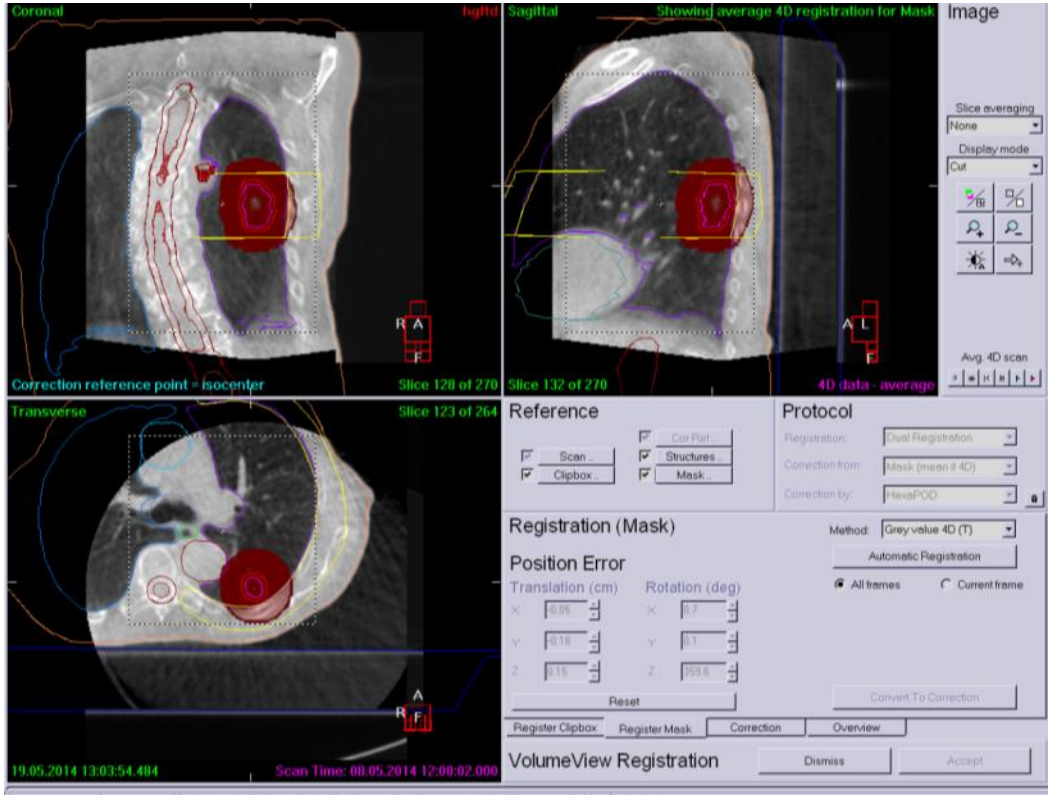

Rotation and translation corrected by:
Robotic Couch 6-D: **Hexapod**

Baseline shift

The measured tumor trajectory was averaged (time-weighted) to quantify displacements of the mean tumor position. Corrections for **baseline shifts** were validated.

Abdominal compression was effective for reducing the amplitude of tumor motion. However the use of abdominal compression seemed to increase the **interfraction variation** in tumor position, despite reducing lung tumor motion. The daily tumor position deviated more systematically from the tumor position in the planning CT. Therefore, **target matching is required to correct or minimize the interfraction variation**.

Thank you!